The European Zoological Journal

ISSN: 2475-0263 (Online) Journal homepage: www.tandfonline.com/journals/tizo21

Spiny bears: a new species of *Ramazzottius* (Eutardigrada: Ramazzotidae) from Mexico unveils a hidden clade within the genus

J. Romero-Mendoza, S. Brandoli, R. Guidetti, J. Vincenzi, D. Hérnandez-Mena, M. Cesari, R. Mata-López & G. Rivas

To cite this article: J. Romero-Mendoza, S. Brandoli, R. Guidetti, J. Vincenzi, D. Hérnandez-Mena, M. Cesari, R. Mata-López & G. Rivas (2026) Spiny bears: a new species of *Ramazzottius* (Eutardigrada: Ramazzotidae) from Mexico unveils a hidden clade within the genus, The European Zoological Journal, 93:1, 503-526, DOI: 10.1080/24750263.2026.2635810

To link to this article: https://doi.org/10.1080/24750263.2026.2635810

Published online: 27 Mar 2026.

THE EUROPEAN ZOOLOGICAL JOURNAL
2026, VOL. 93, NO. 1, 503–526
https://doi.org/10.1080/24750263.2026.2635810

Spiny bears: a new species of *Ramazzottius* (Eutardigrada: Ramazzotidae) from Mexico unveils a hidden clade within the genus

J. Romero-Mendoza [a,b], S. Brandoli [c,d], R. Guidetti [d], J. Vincenzi [d], D. Hérnandez-Mena [e], M. Cesari [d], R. Mata-López [b] and G. Rivas [b]

[a]Posgrado en Ciencias Biológicas, Universidad Nacional Autónoma de México, Mexico City, Mexico; [b]Facultad de Ciencias, Universidad Nacional Autónoma de México, Mexico City, Mexico; [c]Department of Environmental Sciences, Informatics, and Statistics, University Ca' Foscari of Venice, Venice, Italy; [d]Department of Life Sciences, University of Modena and Reggio Emilia, Modena, Italy; [e]Instituto de Biología, Universidad Nacional Autónoma de México, Mexico City, Mexico

ABSTRACT

Species description constitutes a fundamental endeavour, as it lays the foundation for subsequent disciplines which require precise identifications. Nevertheless, species must be regarded as hypothetical constructions requiring validation through diverse lines of evidence. Most of the *Ramazzottius* species were described with limited information according to contemporary standards, underscoring the need to integrate morphological and molecular data in new species descriptions. This study presents the first new species of *Ramazzottius* from Mexico found in lichen samples. Morphological assessment comprised light and electron microscopy imaging as well as linear morphometrics. Uncorrected *p*-distance calculations, Assemble Species by Automatic Partitioning (ASAP), and Poisson Tree Processes (PTP) were applied for molecular species delimitation, using the genes COI and ITS-2. Additionally, phylogenetic relationships within the genus *Ramazzottius* were reconstructed through maximum likelihood and Bayesian inference approaches, concatenating fragments of four genes: 18S, ITS-2, 28S and COI. The new species *Ramazzottius suzithuae* sp. nov. exhibits morphological similarity to *Ramazzottius belubellus* but is distinguished by a particular arrangement of the spines on the dorsal cuticle. All delimitation analyses confirm the molecular distinctiveness of the new species and the existence of at least two species within "*Ramazzottius* cf. *saltensis*". The multi-locus tree recovered five major clades and positions the new species close to these *Ramazzottius* cf. *saltensis* species in their own clade, separated from the "*baumanni*" species grouped in another clade. The lack of complete and consistent diagnostic traits for all these clades still prevents the erection of separate genera.

http://www.zoobank.org/urn:lsid:zoobank.org:act:6D0A7409-8282-41A9-8CF2-1F418EE85F

ARTICLE HISTORY
Received 28 November 2025
Accepted 18 February 2026

KEYWORDS
"baumanni" complex; integrative taxonomy; Mexico; *Ramazzottius*; species delimitation

Introduction

Describing species is the most fundamental task to better know the biodiversity of this world, especially in case of poorly studied taxa. It also lays the foundation for any other discipline that intends to focus on them as models or resources, as it requires accurate identification of the studied species (Gąsiorek et al. 2018). However, it is always important to consider species as hypotheses that are based on different lines of evidence (Pante et al. 2015). Traditionally, the first line comes from morphology; however, the need to go further has been emphasized to give better precision and certainty to descriptions (Padial et al. 2010; Goldstein & DeSalle 2011). Nevertheless, there are biological groups that still require these integrative studies, such as the tardigrade genus *Ramazzottius* Binda and Pilato 1986.

Most of the species within this genus were described decades ago with limited information compared with current standards (Guidetti et al. 2022), raising the question of whether subsequent morphological records additional to their *locus typicus* are valid. In this sense, it is likely that many records, such as *Ramazzottius oberhaeuseri* (Doyère 1840) or *Ramazzottius baumanni* (Ramazzotti 1962), which are the only

CONTACT G. Rivas gerardorivas@ciencias.unam.mx Facultad de Ciencias, Universidad Nacional Autónoma de México, Mexico City 04510, Mexico

species allegedly recorded in Mexico (Beasley 1972; Moreno-Talamantes et al. 2019; López-Sandoval et al. 2025), correspond to false cosmopolitan records (Ugarte & Garraffoni 2024), or belong to species complexes (Kaczmarek et al. 2014; Dey et al. 2023). This situation is clearly exemplified in Europe, where records of *R. oberhaeuseri*, the nominal species of the family Ramazzottidae, masked eight pseudocryptic species distributed in different European countries (Stec et al. 2018).

The validity of the genus *Ramazzottius*, currently including 32 species (Guidetti & Bertolani 2005; Degma & Guidetti 2025; Polishchuk et al. 2025) is supported by molecular evidence; however, only seven of the species are properly delineated by integrative taxonomy – namely, *Ramazzottius claudii* Vecchi and Stec 2024; *Ramazzottius groenlandensis* Kihm et al. 2023; *Ramazzottius kretschmanni* Guidetti et al. 2022; *Ramazzottius oberhaeuseri* (Doyère 1840); *Ramazzottius sabatiniae* Guidetti et al. 2019; *Ramazzottius subanomalus* (Biserov 1985); *Ramazzottius varieornatus* Bertolani and Kinchin 1993.

Even though the number of available sequences of the genus has recently increased, representing the suggested "*baumanni*" and "*szeptycki*" complexes, these species and populations were only partially described, emphasizing the dorsal cuticle characters (Dey et al. 2023) but neglecting any further description of other characters and measurements of animals, as well as lacking information on the egg morphology.

Ramazzottius has been recorded all around the world in diverse microhabitats, such as various species of mosses, lichens, soil, several types of leaf litter (Kaczmarek et al. 2014; McInnes et al. 2017; Guidetti et al. 2019; Michalczyk et al. 2022) and even rock pools (Vecchi & Stec 2024). However, in Mexico only mosses and lichens have been explored; hence, many microhabitats, vegetation types, and biogeographic provinces have yet to be sampled. Therefore, the present study aimed to increase the knowledge of the genus in Mexico, delimiting a new species found in the state of Querétaro through integrative taxonomy and showing its phylogenetic affinities and providing an updated multi-locus phylogeny for the genus.

Materials and methods

Extraction, imaging and morphological analysis of tardigrades

The specimens were found in a lichen sample collected in January 2017 by Jorge Jiménez, southeast from the "Campo Deportivo de Camargo" in Peñamiller, Querétaro (21°06´17.1"N, 99°43´22.9"W). The extraction was carried out by rehydrating fragments of the lichen with tap water for at least 2 h. The wet lichen was examined for tardigrades, which were mostly located on the underside of the lichen, among its rhizines. After soaking the sample, the remaining water was examined under a stereomicroscope, and the animals and eggs were mounted on slides in Hoyer's liquid. A portion of these specimens were mounted in group in 2017 and posteriorly remounted individually in 2024 as a requirement to be accepted in the Tardigrada Collection associated with the Colección Nacional de Ácaros, Instituto de Biología, Universidad Nacional Autónoma de México (UNAM). The unmounting procedure consisted in a simple immersion into tap water for 24 h or until the mounting medium was softened enough to slide the coverslip. Animals and eggs were then recovered and washed in clean water before individual mounting.

Observations with light microscopy (LM) were carried out under phase contrast (PhC) and bright field (BF) up to the maximum magnification (100× oil objective) with a Nikon Eclipse E200 equipped with a Lumenera Infinity 1 digital camera, at the Instituto de Biología, UNAM. Males were detected by the presence of spermatids and spermatozoa within the gonads and gonoducts in animals mounted in Hoyer's liquid.

Roman numerals, previously used for the localization of gibbosities (Michalczyk & Kaczmarek 2010), are employed here to designate the body segmentation, coinciding with the cuticular folds observed from the head to the fourth pair of legs. Following this criterion, segment I is located anterior to the elliptic organs and segment X just before the hind legs (see Figure 1).

Linear morphometric data of taxonomically relevant structures were handled with a modified "Parachela" v. 1.8 template available on the Tardigrada Register website (Michalczyk & Kaczmarek 2013). All measurements were taken in micrometres (µm). Body length was measured from the anterior extremity to the posterior end of the body, excluding the hind legs. Buccal tube length and the level of the stylet support insertion point were measured according to Pilato (1981). In the morphometry of the class Eutardigrada, the *pt* value is the relationship between the length of a given structure and the length of the buccal tube,

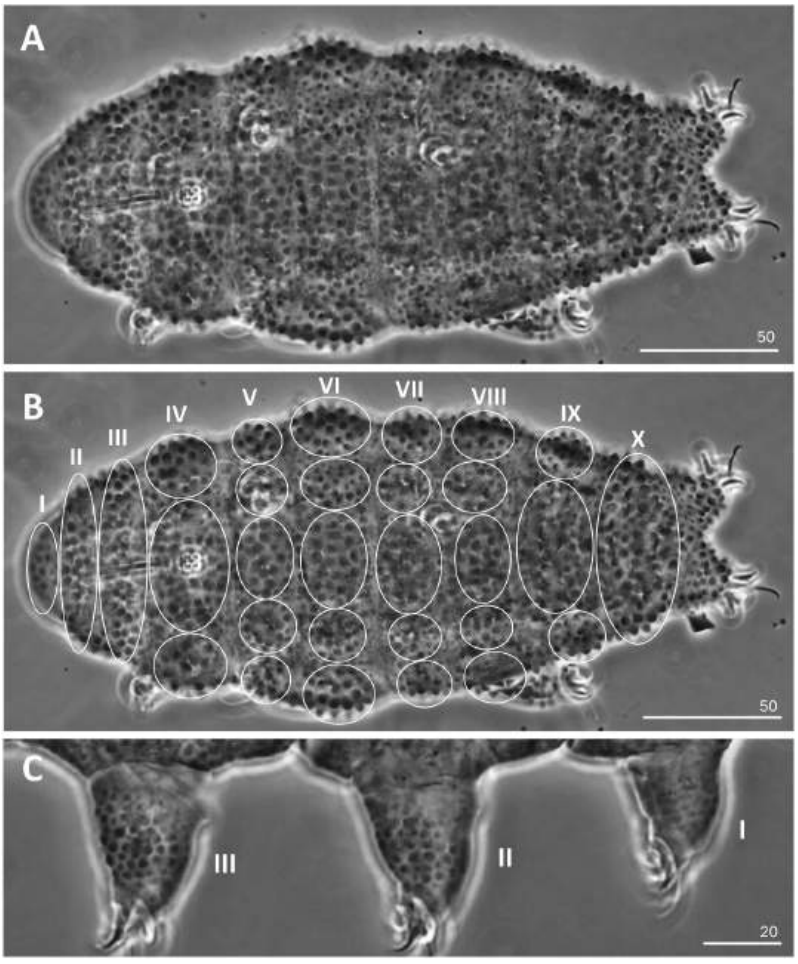

Figure 1. *Ramazzottius suzithuae* sp. nov. A, dorsal view of the body. B, the same dorsal view as a with Roman numerals (I–X) indicating the body segments (transversal bands) and ellipses highlighting the arrangement of the sculpturing present on each segment. C, smaller tubercles (sometimes referred to as granulation) present dorsally on legs I–III. All Phase Contrast. The number above each scale line corresponds to its length in µm.

expressed as a percentage (Pilato 1981). Claws were measured according to Beasley et al. (2008). Egg measurements were taken according to Kaczmarek and Michalczyk (2017).

Additional specimens and eggs were extracted from the sample for scanning electron microscopy (SEM) observation and processed with the A2 (boiling EtOH + EtOH drop) protocol standardized by Camarda et al. (2024). Specimens were mounted on stubs and sputter coated with a thin layer of gold. The observations and images were acquired with a JEOL JSM6360LV Scanning Electron Microscope at the Instituto de Ciencias del Mar y Limnología, UNAM.

DNA extraction and sequencing

Prior to DNA extraction, 10 specimens and 4 eggs were temporarily mounted in water on a glass slide and examined under LM to confirm identification and obtain photogenophores. DNA was extracted from individual specimens and eggs using the HotSHOT technique (Truett et al. 2000), modified by Montero-Pau et al. (2008): each specimen was placed in a 0.2 mL polymerase chain reaction (PCR) tube with 12.5 µL of alkaline lysis buffer (NaOH 25 mM, disodium Ethylenediaminetetraacetic (EDTA) 0.2 mM, pH 8.0) and incubated at 95°C for 30 min. The tubes were then placed in a refrigerator at 4.0°C for 5 min. After that, an additional 12.5 µL of a neutralizing solution (Tris-HCl 40 mM, pH 5.0) was added to the tube. The samples were briefly vortexed, centrifuged, and stored at −20°C.

Table 1. Primers and references for the specific protocols for amplification of the four DNA fragments sequenced in the present study.

DNA fragment	Primer name	Primer direction	Primer sequence (5′–3′)	Primer source	PCR programme
18s	18S_Tar_1Ff	Forward	AGGCGAAACCGCGAATGGCTC	Stec et al. (2017)	Stec et al. (2020)
	18S_Tar_1Rr	Reverse	GCCGCAGGCTCCACTCCTGG		
28s	28S_Eutar_F	Forward	ACCCGCTGAACTTAAGCATAT	Gąsiorek et al. (2018)	
	28SR0990	Reverse	CCTTGGTCCGTTTTTCAAGAC	Mironov et al. (2012)	
	391	Forward	AGCGGAGGAAAAGAAACTAA	Nadler and Hudspeth (1998)	Hernández-Mena et al. (2022)
	536	Reverse	CAGCTATCCTGAGGGAAAC	Stock et al. (2001)	
ITS	BD1	Forward	GTCGTAACAAGGTTTCCGTA	Luton et al. (1992)	
	BD2	Reverse	TATGCTTAAATTCAGCGGGT		
COI	COI_Ram_F3	Forward	CGCTCAAYTDAGHGAACC	Stec et al. (2018)	Michalczyk et al. (2012)
	COI_Ram_R2	Reverse	ACTTCWGGRTGDCCAAARAATCA		
	LCO	Forward	GGTCAACAAATCATAAAGATATTGG	Folmer et al. (1994)	
	HCOoutout	Reverse	GTAAATATATGRTGDGCTC	Prendini et al. (2005)	

Fragments of four DNA markers were amplified (for PCR primers and protocols see Table 1): one mitochondrial, the cytochrome c oxidase subunit I (COI); and three nuclear, the small ribosome subunit (18S rRNA), the large ribosome subunit (28S rRNA) and the complete internal transcribed spacer region (ITS1 + 5.8S+ITS-2). The PCR reaction volume was prepared according to Hernández-Mena et al. (2022), and the products were controlled by 1.0% agarose gel electrophoresis stained with GelRed Nucleic Acid Gel Stain, 10000X (Biotium™). The sequencing reaction was prepared with 4 µL of water, 2 µL of Buffer 5X, 2 µL of Big Dye Terminator v. 3.1 (Applied Biosystems), 1 µL of the primer and 2.5 µL of the purified product. The reaction was placed on a PCR 2720 with the manufacturer's suggested protocol schedule. At the end, the PCR products were purified with Sephadex CentriSep™ plates (Princeton) and read in a 3730xl sequencer (Applied Biosystems), at LANABIO, UNAM.

Molecular characterization and alignment

The identity of the sequences obtained was first verified using the Basic Local Alignment Search Tool (Altschul et al. 1990). Then, chromatograms were inspected with FinchTV 1.4.0 (https://digitalworldbiology.com/FinchTV) for the presence of ambiguous bases. Final nucleotide sequences were aligned with the MAFFT algorithm (Katoh et al. 2002) as implemented in the EMBL-EBI Job Dispatcher sequence analysis tools framework (Madeira et al. 2024; https://www.ebi.ac.uk/jdispatcher).

Alignments were visually inspected, trimmed, and analysed for uncorrected genetic *p*-distances using MEGA7 (Kumar et al. 2016). Due to the very gappy alignment and the numerous ambiguous bases present in sequences from the "*baumanni*" and "*szeptycki*" complexes, pairwise deletion of gaps/missing data was chosen in computing the genetic distances for the ITS-2 marker. The COI sequences were translated to amino acids using the invertebrate mitochondrial code implemented in the same software, to check for the presence of stop codons and therefore of pseudogenes. The final alignments, including sequences available on National Center for Biotechnology Information (NCBI), were constituted as follows:

- 124 COI sequences of the genus *Ramazzottius* available from NCBI, trimmed to 576 bp. The sequence of *Ramazzottius* cf. *saltensis* AR.365.01 from "near Uruguay River", Argentina, was excluded from subsequent analyses due to its extremely divergent sequence, producing a disproportionately long branch.
- 295 ITS-2 sequences of the genus *Ramazzottius* available from NCBI, trimmed to 483 bp, were used for exploration. Given that extremely long branches, as well as unbalanced over-sampled species, can affect inferences (Zhang et al. 2013; Magoga et al. 2021; Yin et al. 2023), the disproportionately longest-branched sequences within a given clade were excluded and only 12 specimens of *Ramazzottius*. sp. 1 and eight of *Ramazzottius* sp. 2 from Denmark (Gąsiorek et al. 2024) were considered, resulting in a final alignment with 91 sequences.
- The final alignment of the Large ribosome SubUnit (LSU) rRNA consists of 61 sequences trimmed to 663 bp. Sequences of *Ramazzottius sabatiniae* Guidetti et al. 2019, *R*. sp. from Niva and *R*. sp. TarCPH31 from Sweden were excluded since they correspond to ulterior regions of the marker.

– The Small ribosome SubUnit (SSU) rRNA alignment encompasses 78 sequences trimmed to 789 bp. Sequences of *Ramazzottius* sp. TarCPH31 from Sweden and *R.* "*oberhaeuseri*" from France were excluded due to the short overlapping fragments in the trimmed alignment and their inconsistent position in preliminary tree topologies.

Phylogenetic inference and species delimitation

The four DNA markers were concatenated using the software Concatenator (Vences et al. 2021, 2022) to construct a matrix of 200 sequences, 2508 bp long. Sequences of *Hebesuncus conjugens* (Thulin 1911) generated by Vecchi and Stec (2024) were used to root the phylogenetic tree. After exploration analyses, the matrix was thinned to 114 sequences, excluding specimens with only one conservative marker (18S or 28S) and most of the single-sequence representatives of each species. Accession numbers of the remaining sequences in this matrix (representing the final dataset used for the phylogenetic analyses) are given as supplementary material (Supporting information S1).

Model selection (Kalyaanamoorthy et al. 2017; Supporting information S2) and maximum likelihood (ML) phylogenetic reconstruction with the IQTREE algorithm (Nguyen et al. 2015) were performed on the IQTREE web server (Trifinopoulos et al. 2016; http://iqtree.cibiv.univie.ac.at/) with the parameters pers = 0.3 and numstop = 500 as recommended in the web server for data with short sequences, an ultrafast bootstrap (Hoang et al. 2018) with 5000 replicates, as well as a partition scheme (Chernomor et al. 2016) for the three codon positions of the COI and the concatenated four markers.

The Bayesian inferences (BI) were carried out in MrBayes 3.2.7 (Ronquist et al. 2012). The analyses consisted of 30 million generations, sampling a tree every 1000 generations and discarding the first 25% as burn-in. Evolutionary models used for BI are given in Supporting information S2.

Visualization and primary edition of all the trees was conducted in FigTree (Rambaut 2007). Exported SVG images of each tree were then edited in Inkscape (Inkscape Project 2020) to depict the Primary Species Hypothesis (PSH) schemes of each species delimitation analysis in a single tree and to highlight the clades and subclades recovered in the multi-locus phylogeny.

Molecular analyses for species delimitation were performed using two different single-locus methods. Only the COI and ITS-2 markers were used for these analyses. The first was a distance-based method (Assemble Species by Automatic Partitioning (ASAP); Puillandre et al. 2021), performed on https://bioinfo.mnhn.fr/abi/public/asap/. Second, we used a tree-based method (Bayesian Poisson Tree Processes (bPTP); Zhang et al. 2013) conducted on the webserver (http://species.h-its.org/ptp), with 500,000 Markov chain Monte Carlo (MCMC) generations, thinning the set to 100, discarding the outgroup and the first 25% as burn-in to search for ML and Bayesian solutions.

Results

Taxonomic account

Phylum **Tardigrada** Doyère 1840

Class **Eutardigrada** Richters, 1926

Order **Parachela** Schuster, Nelson, Grigarick and Christenberry, 1980

Superfamily **Hypsibioidea** Pilato, 1969

Family **Ramazzottiidae** Sands, McInnes, Marley, Goodall-Copestake, Convey and Linse, 2008

Genus ***Ramazzottius*** Binda and Pilato 1986

http://www.zoobank.org/urn:lsid:zoobank.org:act:6D0A7409-8282-41A9-8CF2-1F418EE85F

***Ramazzottius suzithuae* sp. nov.**

Holotype. Slide CNAC-TTar000525

Paratypes. 30 animals and 6 eggs mounted on slides, 12 animals and 1 egg mounted on stubs for SEM observation.

Type repositories. Holotype, 25 paratypes and 5 eggs deposited in the Tardigrada Collection associated with the Colección Nacional de Ácaros of the Instituto de Biología, UNAM (CNAC-TTar000500-530); 4 paratypes and 1 egg deposited in the Bertolani collection, University of Modena and Reggio Emilia (Italy).

Type locality. Lichen growing on tree bark, Camargo, Querétaro, Mexico. 21°06´17.1"N, 99°43´22.9"W, 1895 m asl.

The new species was found along with *Macrobiotus* sp. *Milnesium* sp. 1, *Milnesium* sp. 2, *Minibiotus* sp. and *Ramazzottius* aff. *oberhaeuseri* sp. 7 (PX064187, PX071482-87; Table 2).

Etymology

According to a legend of the Otomi (a native culture in Mexico, with large representation in the state of Querétaro), the dark supernatural entity Suzithû was the one who gave plants their spines from her hair to defend themselves from the voracious humans. Since both the animals and eggs appear "spiny", the species name (a Latin patronym in genitive) honours Suzithû, as if these tardigrades were gifted with spines by her too.

Description

Animals (morphometric summary in Table 3; raw measurements in Supporting information S3): Cuticle has no pigmentation. Darker epidermic pigmentation on dorsal bands composed of very fine intracellular solid granules (Figure 2A). Purple to pink body cavity cells in dead specimens. Eyes absent. Two elliptical organs are present on dorso-lateral sides of the head (segment II), visible under both LM and SEM (Figure 2(C,D)). Dorsal cuticle strongly sculptured with very evident sharp conical tubercles (also called spines), arranged in 10 transversal bands corresponding to the body segmentation; only minute granules are present between these segments (Figures 1A, 3(A–C)). In addition, tubercles on bands IV–IX are grouped in round patches (faint gibbosities) that decrease in size radially (Figure 3(D–F)) and are longitudinally aligned along lateral bands at each side of the body and in one wider central band (Figure 3(A–C)); the configuration of these patches is VI: 3–5-5–5-5–3. The dorsomedial patch on segments IV, VI and VIII appears slightly less marked in some specimens (Figure 3(A–B)). Smaller specimens have the sharpest and most marked tubercles (Figure 3(A,D)), while bigger specimens have fewer sharp tubercles, almost hemispherical in several specimens (Figure 3(E,F)), which could lead to confusion with *R. baumanni*. The surface of the spines' bases is covered with nanogranulation (Figure 2B; note that it is much smaller than 1 µm).

Six peribuccal lobes are present around the antero-ventral mouth opening (Figure 4A lower left). Buccopharyngeal apparatus of the *Ramazzottius* type (Figure 4A). Oral cavity armature visible under PhC as only one row composed of two granular teeth, located in the posterior oral cavity (Figure 4A, upper left). Apophyses for the insertion of stylet muscles (AISM) in the shape of blunt hooks and asymmetrical in size and shape with

Table 2. Specimens and GenBank accession numbers of the molecular markers obtained for the two *Ramazzottius* species found in this study.

Taxon	Specimens	18s	ITS	28s	COI
Ramazzottius suzithuae sp. nov	*Ramazzottius*_sp_MXQT_Camargo_R2	PV623147	PV623151	PV623143	PV576544
	*Ramazzottius*_sp_MXQT_Camargo_D1				PV576545
	*Ramazzottius*_sp_MXQT_Camargo_D2	PV623149	PV623152	PV623144	PV576546
	*Ramazzottius*_sp_MXQT_Camargo_D3	PV623150		PV623145	PV576547
	*Ramazzottius*_sp_MXQT_Camargo_D4			PV623146	
	*Ramazzottius*_sp_MXQT_Camargo_D5				PV576548
	*Ramazzottius*_sp_MXQT_Camargo_Egg1	PV623148			
Ramazzottius aff. *oberhaeuseri* sp. 7	*Ramazzottius*_sp_MXQT_CamargoL3c_R1	PX071483	PX071482	PX071486	PX064187
	*Ramazzottius*_sp_MXQT_CamargoL3c_R4			PX071487	
	*Ramazzottius*_sp_MXQT_CamargoL3c_Egg4	PX071485			
	*Ramazzottius*_sp_MXQT_CamargoL3c_J1	PX071484			

Table 3. Morphometric summary of animals of *Ramazzottius suzithuae* sp. nov.

		RANGE		MEAN		SD	
CHARACTER	N	µm	*pt*	µm	*pt*	µm	*Pt*
Body length	30	109 – 294	*605 – 996*	226	*866*	57	*106*
Buccopharyngeal tube							
Buccal tube length	28	17.2 – 31.5	–	25.9	–	4.3	
Stylet support insertion point	29	7.8 – 17.8	*45.1 – 61.2*	14.9	*56.9*	2.5	*2.9*
Buccal tube external width	28	1.3 – 2.4	*6.4 – 9.0*	2.0	*7.6*	0.3	*0.5*
Buccal tube internal width	23	0.5 – 1.0	*2.6 – 3.9*	0.8	*3.1*	0.1	*0.3*
Placoid lengths							
Macroplacoid 1	28	1.4 – 3.0	*7.6 – 10.9*	2.3	*8.7*	0.5	*0.8*
Macroplacoid 2	28	1.3 – 2.8	*6.9 – 9.5*	2.0	*7.7*	0.4	*0.7*
Macroplacoid row	28	3.2 – 6.3	*18.0 – 23.6*	5.1	*19.6*	1.0	*1.3*
Mac2/Mac1	28	79.8 – 99.3		88.9		4.2	
Claw 1 heights							
External base	16	5.1 – 9.9	*25.0 – 36.6*	7.9	*30.1*	1.5	*3.1*
External primary branch	24	5.5 – 13.2	*30.8 – 45.8*	9.3	*37.1*	2.2	*3.6*
External secondary branch	17	4.3 – 8.3	*20.6 – 28.7*	6.3	*25.2*	1.2	*2.6*
Internal base	12	4.2 – 7.2	*17.8 – 24.9*	6.2	*22.2*	0.8	*2.0*
Internal primary branch	9	4.8 – 8.0	*21.9 – 30.9*	6.6	*25.4*	1.2	*3.2*
Internal secondary branch	5	4.2 – 6.1	*17.6 – 22.8*	5.2	*20.7*	0.8	*2.2*
Claw 2 heights							
External base	15	5.2 – 10.4	*25.7 – 36.3*	8.2	*30.7*	1.6	*3.2*
External primary branch	25	5.9 – 13.5	*34.6 – 47.1*	10.3	*39.5*	2.1	*3.2*
External secondary branch	10	4.4 – 8.6	*24.0 – 29.2*	6.3	*26.1*	1.5	*1.4*
Internal base	18	4.1 – 8.0	*19.0 – 27.3*	6.2	*23.1*	1.1	*2.5*
Internal primary branch	10	4.0 – 8.5	*19.7 – 31.8*	6.3	*24.8*	1.7	*4.1*
Internal secondary branch	4	4.5 – 7.4	*21.8 – 26.7*	6.4	*24.1*	1.3	*2.3*
Claw 3 heights							
External base	17	5.4 – 10.6	*24.4 – 37.7*	8.3	*30.8*	1.7	*3.8*
External primary branch	25	5.4 – 13.9	*31.2 – 48.3*	10.4	*40.5*	2.3	*4.1*
External secondary branch	17	4.7 – 9.0	*20.3 – 30.1*	6.9	*26.7*	1.6	*2.5*
Internal base	12	3.6 – 7.4	*17.9 – 28.2*	6.0	*22.6*	1.4	*3.0*
Internal primary branch	12	4.9 – 8.3	*21.7 – 31.6*	6.9	*25.3*	1.1	*3.2*
Internal secondary branch	6	4.6 – 7.9	*22.3 – 27.7*	6.6	*24.7*	1.3	*2.5*
Claw 4 lengths							
Posterior base	6	7.6 – 9.9	*29.5 – 33.4*	9.0	*32.0*	0.8	*1.4*
Posterior primary branch	16	7.2 – 14.4	*40.9 – 50.1*	12.6	*45.1*	2.0	*3.0*
Posterior secondary branch	6	5.1 – 9.8	*24.4 – 31.7*	7.8	*28.8*	1.8	*2.7*
Anterior base	7	6.5 – 7.9	*21.3 – 27.4*	7.1	*24.4*	0.5	*2.4*
Anterior primary branch	5	4.8 – 7.6	*25.7 – 28.5*	6.3	*27.4*	1.4	*1.5*
Anterior secondary branch	6	4.5 – 6.7	*22.7 – 27.8*	5.6	*25.4*	1.1	*2.1*

N, number of structures measured; RANGE, smallest to largest structure amongst all measured specimens; SD, standard deviation.

respect to the frontal plane (Figure 4B). Each stylet furca has two wide semispherical condyles laterally flattened and internally sclerified, supported by short branches with large apophyses (Figure 4C). Buccal tube with a posterior bend and thickened walls after the stylet support insertion point. Pharyngeal apophyses triangular, smaller than the two roundish macroplacoids (Figure 4(A,D)). Macroplacoid length configuration 1 > 2. Both macroplacoids have a medial incision (Figure 4D). Microplacoid and septulum are absent.

Claws of the *Ramazzottius* type (*oberhaeuseri* variant according to Guidetti et al. 2019; Figure 5(A,F)). Primary branches of external and posterior claws are long and thin, curved only distally. A non-sclerotized light refracting unit (LRU) is present between the claw base (continuous with the secondary branch) and the primary branch, connected to the base by a thin cuticular filament (Figure 5C). Internal and anterior claws have a different shape than external claws. Accessory points on primary branches of all claws present. Smaller spiny tubercles present on the external portion of all legs, decreasing in size and sharpness in a posterior-to-anterior direction (Figures 1C, 5(B,D,E) similarly, the claws become smaller in a posterior-to-anterior direction (Table 3). Bars and other cuticular thickenings on legs absent.

Eggs (morphometric summary in Table 4; raw measurements in Supporting information S3): laid freely, whitish and spherical. Processes with variable size and shape, ranging from tiny spines to flexible filaments; however, the major part has an intermediate elongated conical shape (Figures 6(A–D), 7(B–D)); a few rare processes have a septate bubble-like internal structure (Figure 6A). The surface between processes densely dotted under PhC (Figure 6(A–D)), smooth or slightly lumpy under SEM (Figure 7(B,C)). The processes are irregularly distributed on chorion, so there are several clearings between more widely spaced processes. One

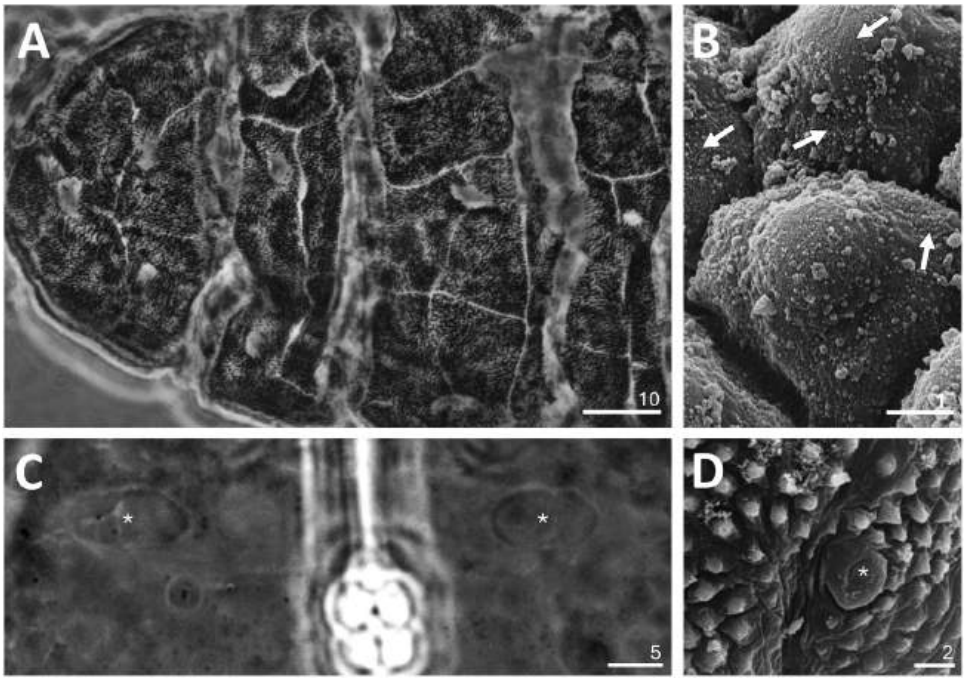

Figure 2. *Ramazzottius suzithuae* sp. nov. A, detail of the dorsal epidermal pigmentation. B, close-up of a group of tubercles to show the nanogranulation (white arrows). C,D, elliptical organs. A, C, Phase Contrast; B, D, Scanning Electron Microscopy. The number above each scale line corresponds to its length in µm.

egg with a fully developed embryo was found (Figure 7A). Females carrying eggs in development (Figure 8A), as well as males with spermatids (Figure 8B) and developed spermatozoa (Figure 8C), were also found. A large papilla is present on the external side of legs IV of some males, although it is not visible on others (Figure 8D, F).

Differential diagnosis

The exact combination of characters from animals and eggs of the new species has not been reported for any other *Ramazzottius* species. However, since many of the descriptions and records of *Ramazzottius* species lack some information, comparisons are held separately.

The cuticular sculpture of the animals (including nanogranulation on the base of tubercles) is similar to that of *Ramazzottius* cf. *baumanni* in Dey et al. (2023, Figure 3A–C) collected in Argentina. The two species have a similar arrangement of strongly sclerotized and conical (rather than hemispherical) tubercles. Nevertheless, since *Ramazzottius* cf. *baumanni* was not properly described (only molecular data and images of the dorsal cuticle were published), a deeper morphological and morphometrical comparison cannot be made for now (although see the molecular characterization for clear distinction).

Ramazzottius suzithuae sp. nov. is also different from other species of the so-called *baumanni* complex, for which eggs are unknown. Particularly, it differs from:

- *Ramazzottius belubellus* Bartels et al. 2011 (compared only with similar sized specimens of *R. suzithuae* sp. nov.), in the arrangement of the dorsal sculpture (spines homogeneously distributed on the entire dorsum in *R. belubellus*, spines grouped in patches from segment IV to segment IX in *R. suzithuae* sp. nov.), a more posterior stylet support insertion point (*pt* range of 55.2–57.1 in *R. belubellus*, *pt* range of 57.3–61.2 in *R. suzithuae* sp. nov.), a wider buccal tube (*pt* of the external width 6.5–7.1 in *R. belubellus*, *pt* of 7.7–9.1 in *R. suzithuae* sp. nov.), a bigger second macroplacoid (*pt* 4.3–6.9 in *R. belubellus, pt* 8.3–9.5 in *R. suzithuae* sp. nov.) and a higher external base of claws I (*pt* of 16.7–20.7 in *R. belubellus*, *pt* of 24.6–30.6 in *R. suzithuae* sp. nov.).
- *Ramazzottius baumanni* (Ramazzotti 1962; recent images in Dey et al. 2023), in the shape of the dorsal tubercles (always semispherical in *R. baumanni*, spines to flattened cones in the new

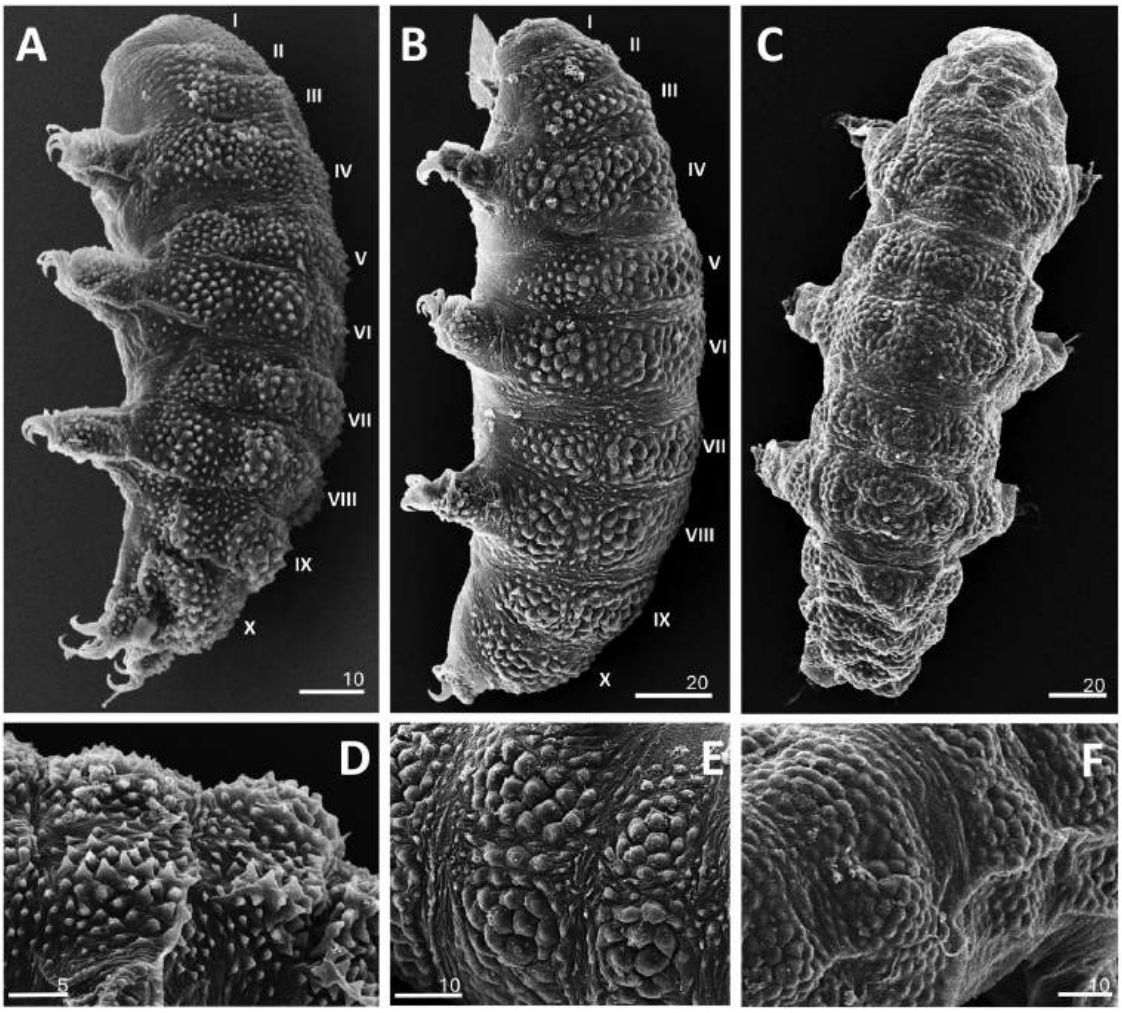

Figure 3. Variation in the tubercles of *Ramazzottius suzithuae* sp. nov. under Scanning Electron Microscopy; Roman numerals (I–X) indicate the same body segments as in Figure 1. A–C, Habit of animals increasing in size. D–F, detail of the tubercles of each animal in A–C, respectively. Notice that the larger the size of the animal, the less sharp its tubercles are. The number above each scale line corresponds to its length in µm.

species), the arrangement of the dorsal sculpture (tubercles homogeneously distributed on the entire dorsum in *R. baumanni*, spines grouped in patches from segment IV to segment IX in *R. suzithuae* sp. nov.) and a subtle difference in the level of sclerotization of the tubercles' apex as seen under PhC (solid black polygons in *R. baumanni*, blurred dark grey polygons in *R. suzithuae* sp. nov.)

– *Ramazzottius syraxi* Polishchuk, Kayastha, Warguła and Kaczmarek 2025, in the coverage of the sculpture on the body (only eight body segments in *R. syraxi*, all 10 body segments in *R. suzithuae* sp. nov.) and legs (absent on all legs in *R. syraxi*, present on all legs in *R. suzithuae* sp. nov.), the configuration of the faint gibbosities (VIII:1–2-3–4-5–4-3–1 in *R. syraxi*, VI: 3–5-5–5-5–3 in *R. suzithuae* sp. nov.) and the shape of the tubercles (pebble-shaped polygonal granules with ragged edges under PhC in *R. syraxi*, spines of sclerotized apex with smooth and blurry edges in *R. suzithuae* sp. nov.).
– *Ramazzottius* cf. *saltensis* (Dey et al. 2023), in the presence of well-developed gibbosities (faint in the new species) and the tubercles constitution (more translucent with wrinkled apex in *R.* cf. *saltensis*, more sclerotized with smooth apex in the new species).

Additionally, *Ramazzottius theroni* Dastych 1993 is not considered within the *baumanni* complex (Dey et al. 2023) despite having a strongly sculptured dorsal cuticle with sclerotized polygons. It differs from

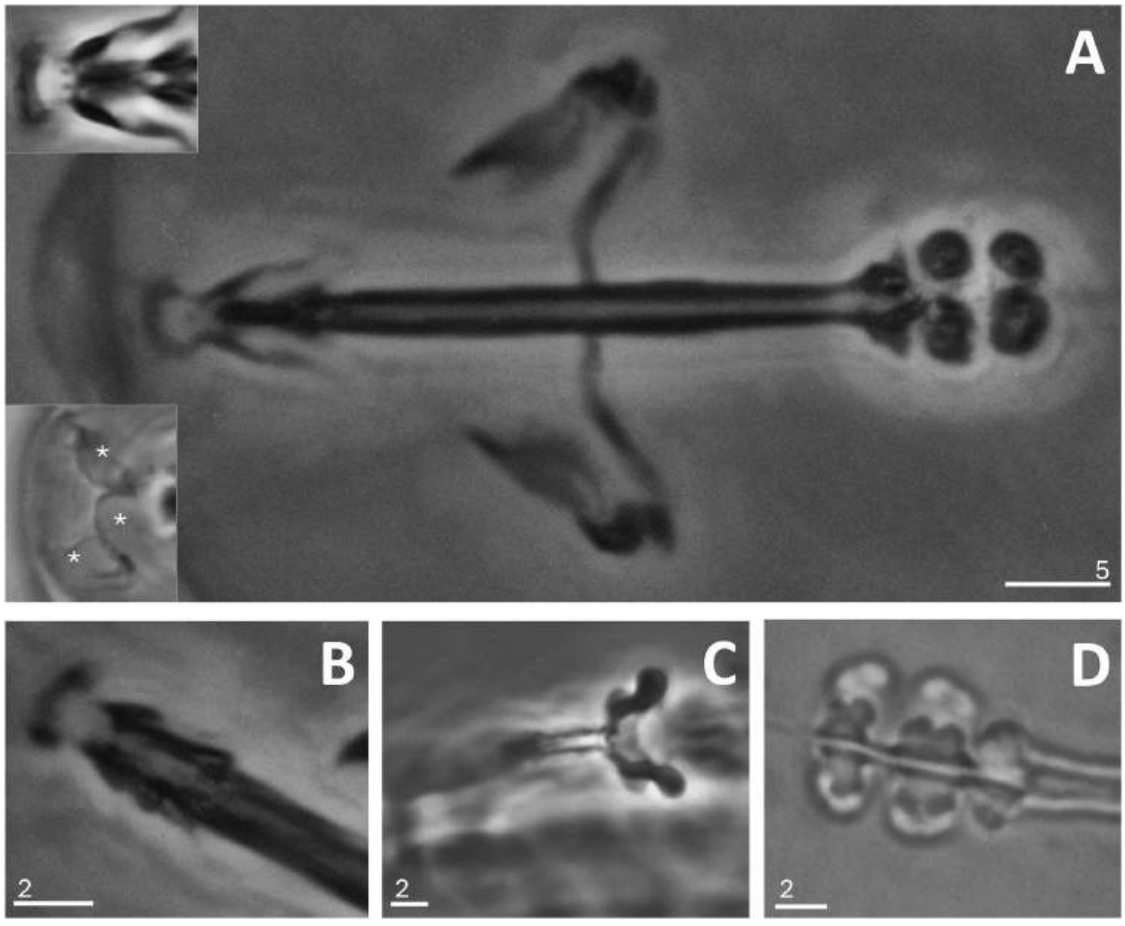

Figure 4. Buccopharyngeal apparatus of *Ramazzottius suzithuae* sp. nov. A, buccopharyngeal apparatus *in toto*; insets show the dorsal band of teeth (above) and the peribuccal lobes (below). B, dorsal and ventral Apophyses for the Insertion of Stylet Muscles (AISM). C, stylet furca. D, upper view of the macroplacoids. A–C, Phase Contrast. D, BF. The number above each scale line corresponds to its length in µm.

R. suzithuae sp. nov. by the presence of eyes (absent in the new species) and sharpness of the cuticle sculpturing (always hemispherical in *R. theroni* vs spines to flattened cones in the new species).

The rest of the known *Ramazzottius* species differ from *Ramazzottius suzithuae* sp. nov. in the absence of strongly sculptured cuticle with elevated "polygons" and sclerotized apices (definition of the *baumanni* complex), but the eggs are similar to six other species having dense punctuation in the egg surface under PhC, differing particularly from:

– *Ramazzottius horningi* Binda and Pilato 1994, in the presence of a crown of dots bigger than chorion punctation around the base of the processes, absent in the new species.
– *Ramazzottius claudii* Vecchi and Stec 2024, in the presence of dots in the egg processes under PhC (egg processes smooth under both, PhC and SEM in the new species) and the absence of tiny processes (mostly medium to large processes in *R. claudii*, tiny to large processes in the new species).
– *Ramazzottius anomalus* (Ramazzotti 1962; recent images in Guidetti et al. 2022), in the shape of the egg processes (aculeus in *R. anomalus*, conical to filamentous in the new species).
– *Ramazzottius groenlandensis* Kihm et al. 2023 in the shape of processes (mostly stumpy with bulbous or concave apices in *R. groenlandensis*, mostly elongated conical and filamentous in the new species).
– *Ramazzottius valaamis* Biserov and Tumanov 1993 (recent images in Guidetti et al. 2022) by the shape of the egg processes (only tiny filaments in *R. valaamis*, mostly large spines or filaments in the new species).

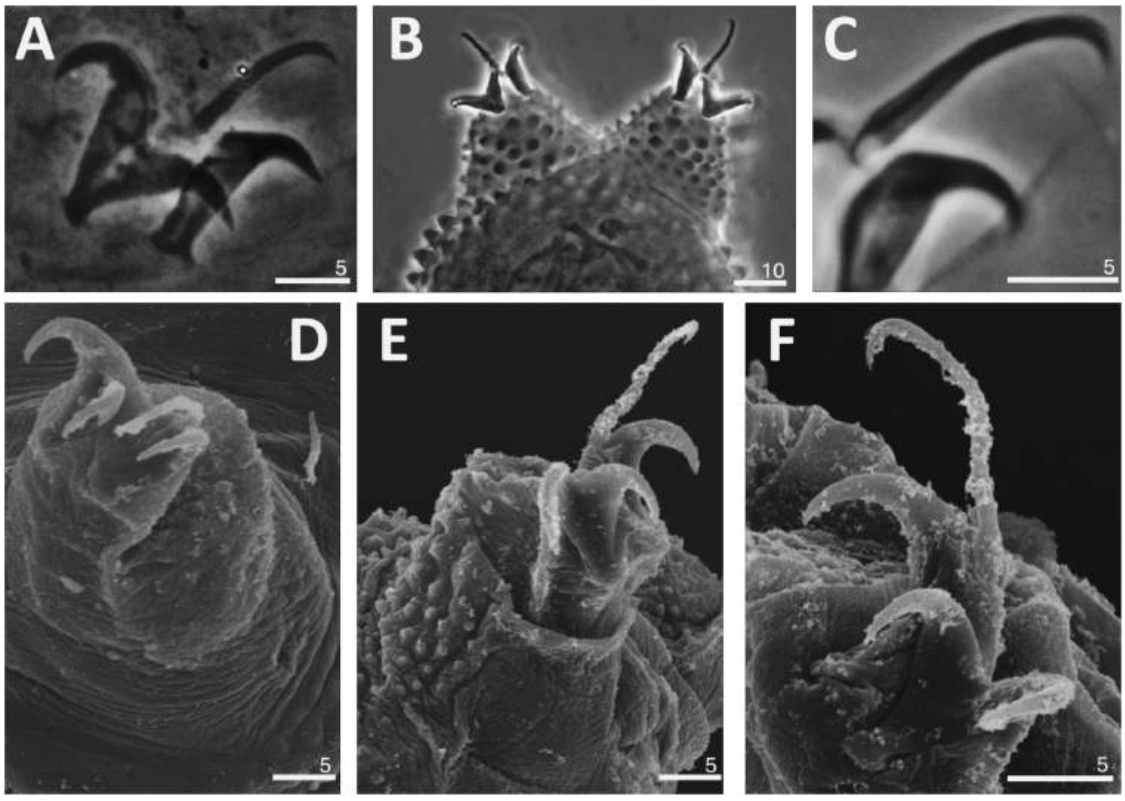

Figure 5. Claws of *Ramazzottius suzithuae* sp. nov. A, claws I. B, claws IV. C, cuticular filament connecting primary branch and claw base. D, leg I with a smooth dorsal portion. E, leg IV with evident tubercles. F, Claws III. A–C, Phase Contrast; D–F, Scanning Electron Microscopy. The number above each scale line corresponds to its length in µm.

Table 4. Measurements (in µm) of morphological structures of the eggs of *Ramazzottius suzithuae* sp. nov.

CHARACTER	N	RANGE			MEAN	SD
Egg bare diameter	4	50.5	–	68.3	59.5	7.3
Egg full diameter	4	65.4	–	85.4	74.6	8.8
Average Processes height	12	6.9	–	11.1	8.7	1.3
Average Processes base width	12	1.6	–	3.4	2.6	1.2
Average processes base/height ratio	12	14%	–	40%	30%	1.4
Inter-process distance	12	1.6	–	6.2	4.3	0.7
Number of processes on the egg circumference	4	16	–	26	19.0	0.5

N, number of eggs/structures measured; RANGE, smallest to largest structure amongst all measured specimens; SD, standard deviation.

– *Ramazzottius varieornatus* Bertolani and Kinchin 1993 by having smaller eggs (bare diameter 69.9–73.3 µm in *R. varieornatus*, 58.9–68.3 µm in the new species) and more irregularly spaced processes (closer together processes in *R. varieornatus*, large clearings without processes in the new species).

Genetic distances

Fifteen sequences of fragments of the regions COI (five), 18S (four) and 28S (four), as well as the complete ITS region (two) were obtained from five animals and one egg of *Ramazzottius suzithuae* sp. nov.; additionally, seven sequences from three animals and one egg of the other *Ramazzottius* species found in the sample were generated for disambiguation (Table 4).

The ranges of uncorrected genetic *p*-distances between other *Ramazzottius* species and within the species population were:

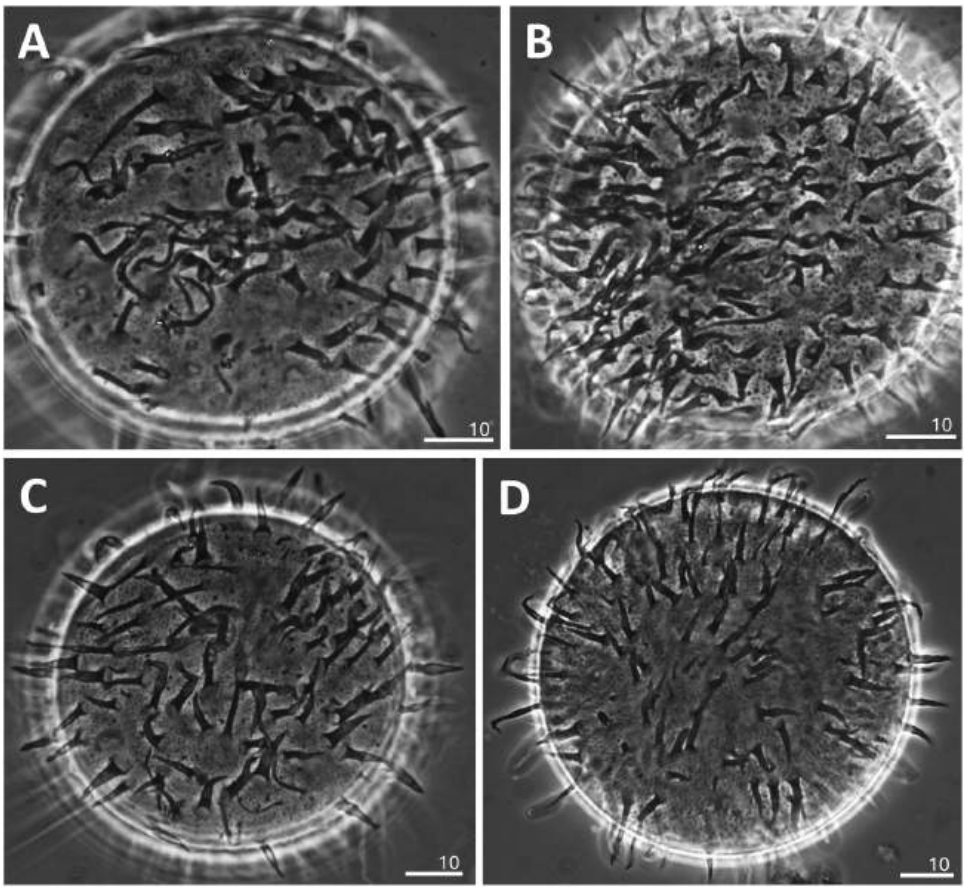

Figure 6. Variability of processes on the eggs of *Ramazzottius suzithuae* sp. nov. All pictures were taken under Phase Contrast. The number above each scale line corresponds to its length in µm.

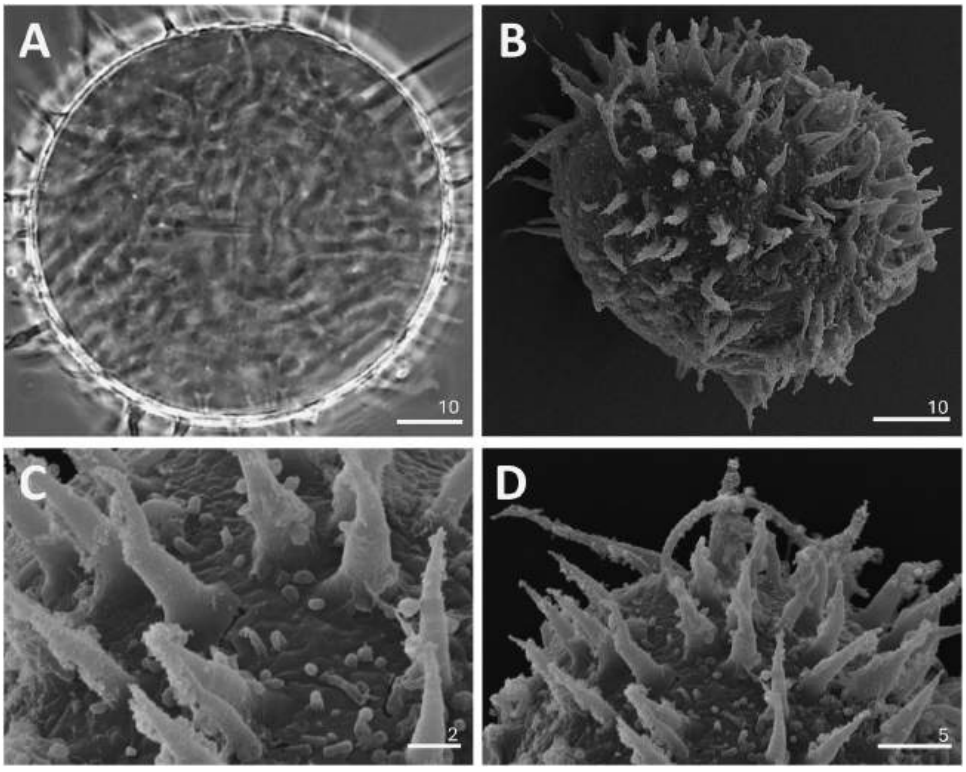

Figure 7. Eggs of *Ramazzottius suzithuae* sp. nov. A, an embryonated egg. B, general view under Scanning Electron Microscopy. C,D, details of the chorion and processes. A, Phase Contrast; B–D, Scanning Electron Microscopy. The number above each scale line corresponds to its length in µm.

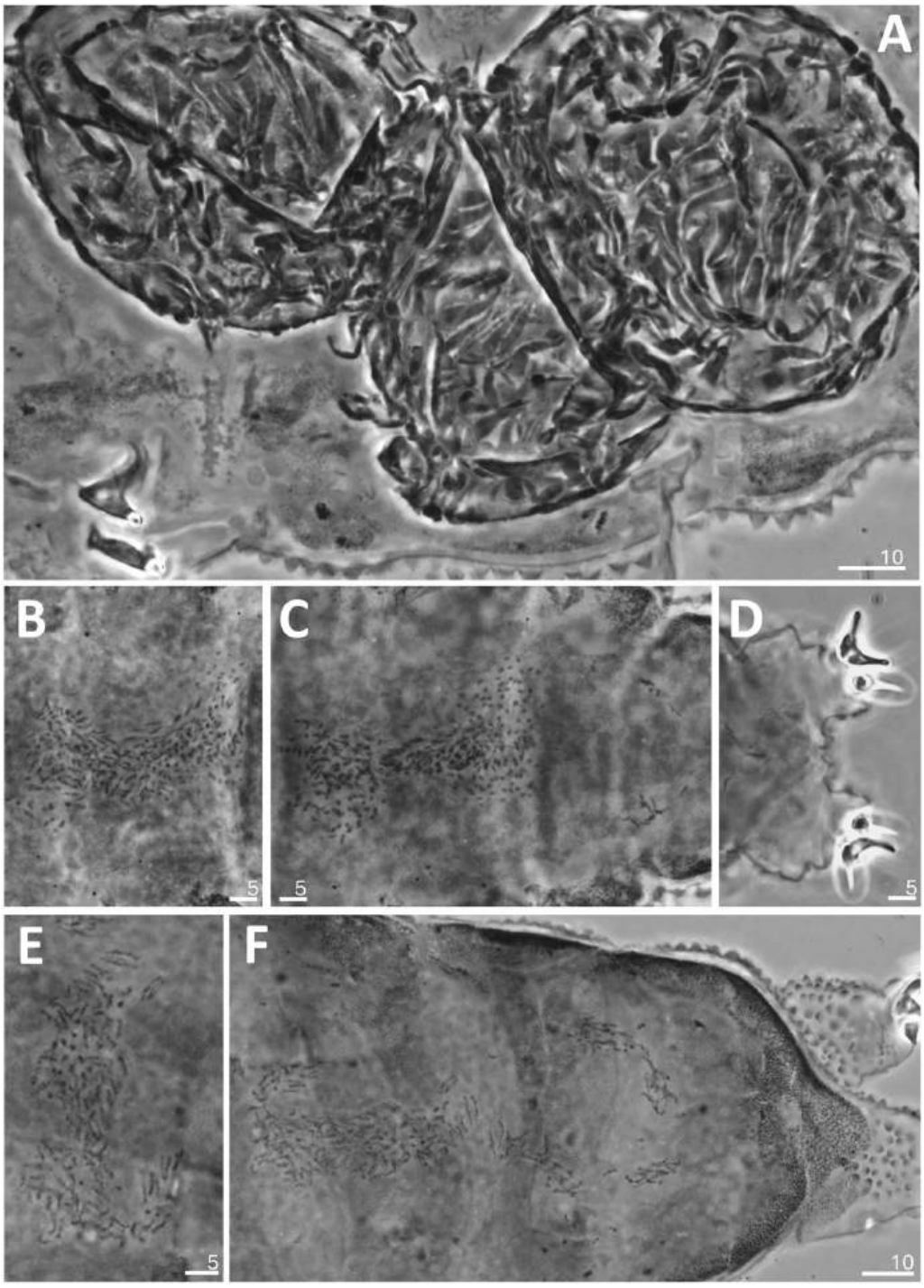

Figure 8. Sexual distinction in specimens of *Ramazzottius suzithuae* sp. nov. A, a female with three eggs. B,C, a male with developing spermatids. D, legs IV of the same male as in B,C showing bulges on the external portion of the legs. E,F, another male with developed spermatozoa, but with no visible bulge on the legs IV. The number above each scale line corresponds to its length in µm.

COI (259 positions in the final data set): intraspecific distances range 0–1.4%; interspecific distances ranged 14.67–21.24%, with the most similar being *Ramazzottius kretschmanni* Guidetti Cesari, Giovannini, Ebel, Förschler & Schill, 2022 from Germany (OM370801-4) and the least similar being *R. oberhaeuseri* (Doyère 1840) from Denmark (PQ356866-7) [Pairwise deletion considering all positions ranged from 15.7% to 20.7%].

18S rRNA (789 positions in the final data set): intraspecific distance was 0%; range of interspecific distances 0.7–13.2%, with the most similar being *Ramazzottius* cf. *saltensis* from near Uruguay River, Argentina (OP930858) and the least similar being *Ramazzottius* sp. from Oregon, USA (JX888523).

ITS-2 (483 positions in the final data set): intraspecific distance was 0%; interspecific distances ranged 16.47–31.27%, with the most similar being *Ramazzottius* cf. *saltensis* from Chaco, Argentina (OP930941) and the least similar being *Ramazzottius* aff. *szeptycki* from South Africa (OP930925).

28S rRNA (663 positions in the final data set): range of intraspecific distances 0–0.2%; range of interspecific distances 2.7–13.9%, with the most similar being *Ramazzottius* cf. *saltensis* from Campiña de América, Argentina (OP930903) and the least similar being *Ramazzottius* aff. *szeptycki* from Bharat (OP930891).

Species delimitation

The validity of *R. suzithuae* sp. nov. is supported by both the ASAP and bPTP analyses for the COI (Figure 9) and ITS-2 regions (Figure 10). Particularly for the COI fragment, ASAP identified 25 PSH at the lowest asap score = 2.5, while bPTP recognizes 28 PSH. The difference lies in the split of *Ramazzottius* cf. *saltensis* from Campiña de América + Near Uruguay River (OP926996–OP927001) and *R.* aff. *oberhaeuseri* sp. 8 (FJ435799, FJ435800) into three and two separate PSH, respectively (Figure 9; accession numbers present in the tree).

Additionally, concordant subsets between ASAP and bPTP are: the divergence of *Ramazzottius szeptycki* sequences from the same South African sample (splitting specimens 131–01 and 131–02 into two different PSH), the split of *R.* cf. *saltensis* from Chaco and Campiña de América + Near Uruguay River into at least two different PSH, the inclusion of a Russian population in *R. oberhaeuseri sensu stricto (s.s.)* and the inclusion of North American populations from USA and Mexico to *Ramazzottius* sp. 7, greatly extending its distribution from the Palearctic (Figure 9).

The COI tree could not recover any clade encompassing *Ramazzottius suzithuae* sp. nov., suggesting a lack of closely related taxa among sequences available to date.

In the case of the ITS-2 region, the results of species delimitation were partially incongruent with respect to the COI delimitations and even known taxonomy. The best ASAP partition identified 22 PSH at the lowest ASAP score = 5, over-splitting previously delimited species (such as *Ramazzottius subanomalus* (Biserov 1985) but at the same time clustering six species, among which are species as different as *Ramazzottius claudii* and *R. oberhaeuseri s.s*. The bPTP analysis recovered 20 PSH, mostly consistent with COI delimitation and current taxonomy, but still lacking the resolution to separate *Ramazzottius varieornatus* from *R.* aff. *varieornatus*. *Ramazzottius suzithuae* sp. nov. was clearly distinguished from any other species in both approaches and is positioned in a well-supported clade with the two *R.* cf. *saltensis* species (Figure 10; accession numbers present in the tree).

Otherwise, the delimitation with a complete ITS-2 alignment (295 sequences) yielded highly irrational partitions, such as 28–36 species for ASAP and 40–101 species for bPTP, showing the sensitivity of these analyses to over-sampled species.

Multi-locus phylogeny

The phylogenetic analyses of the thinned alignment with four concatenated markers consistently recovered five major clades and one ambiguous clade (called clade X; Figure 11) which are also recovered from the full alignment before thinning, the ITS-2 + 18S + 28S matrix and partially from COI +18S + 28S and COI+ITS-2 matrices (Supporting information S4.1–5). These clades are described below.

Clade A. Can be subdivided into several clusters: the subclade AA (*R. groenlandensis* + *R.* sp. from Nivaa, DK + *R.* aff. *oberhaeuseri* sp. 1), the subclade AB (*R. varieornatus* + *R. sabatiniae* + *R.* aff. *varieornatus* + *R. claudii*), both clades not well supported; the subclade AC (*R. oberhaeuseri s.s.*), the subclade AD (*R. kretschmanni* + *R.* sp. 3 from Denmark), the not well-supported subclade AE (*R.* aff. *oberhaeuseri* sp. 7 + *R.* aff. *oberhaeuseri* sp. 8) and the subclade AF (*R. subanomalus*+ *R.* aff. *oberhaeuseri* sp. 3). The inclusion of short and conservative single-locus sequences from Ithaca and Alaska in the complete allignment decreased support and obscured different relationships within Clade A (Supporting information S4.1–2).

Clade B. Limited to *Ramazzottius* cf. *baumanni* and *R.* aff. *baumanni* species.

Clade C. Includes the two species previously obscured in *Ramazzottius* cf. *saltensis* as a subclade CA and *R. suzithuae* sp. nov. as subclade CB.

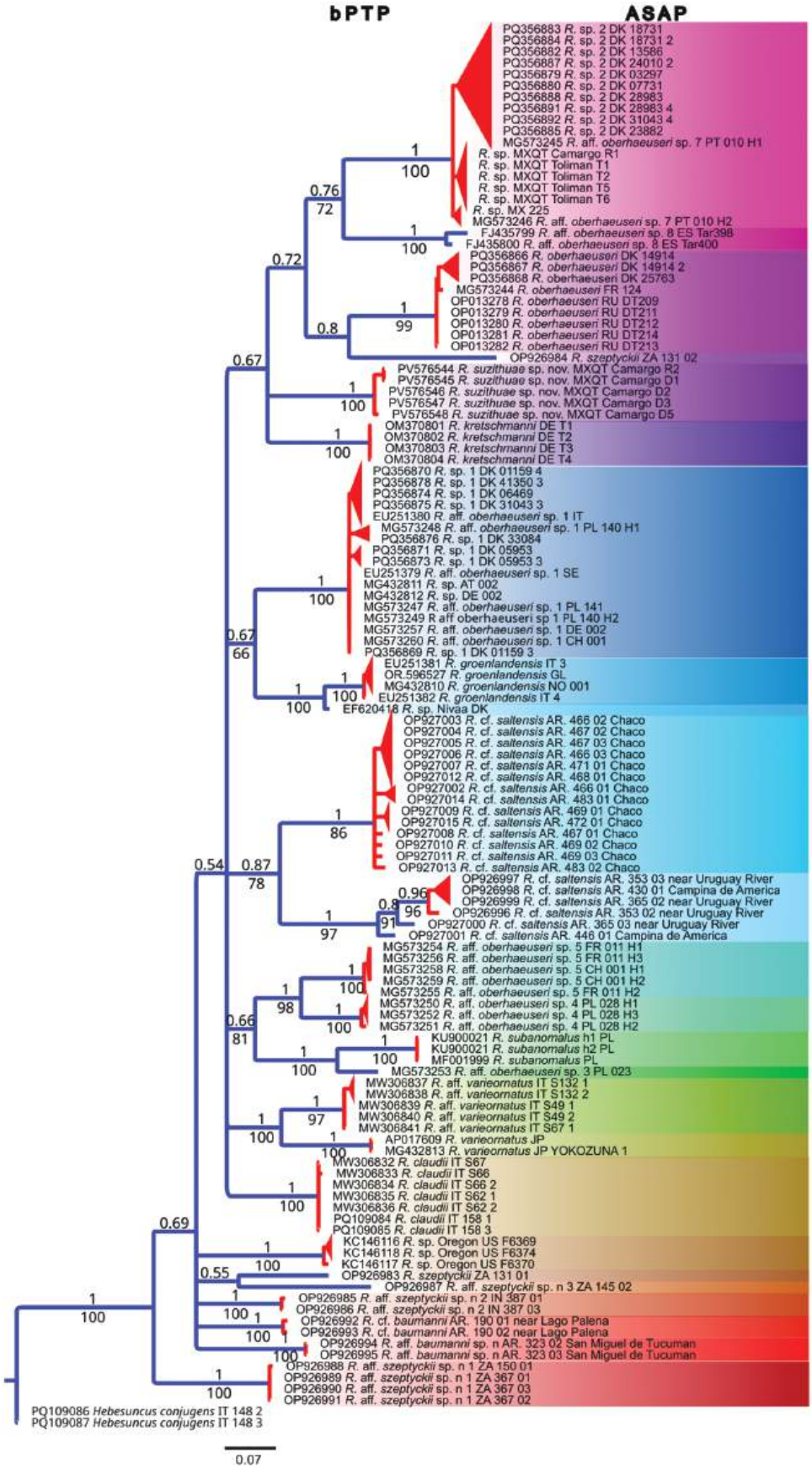

Figure 9. Molecular species delimitation of the COI sequences of the genus *Ramazzottius*. Left: putative species from the PTP analysis are indicated by transitions from blue-coloured branches to red-coloured branches. Right: different coloured sets denote specimens grouped by the best partition of the ASAP analysis. Posterior probability and bootstrap values are shown above and below branches, respectively.

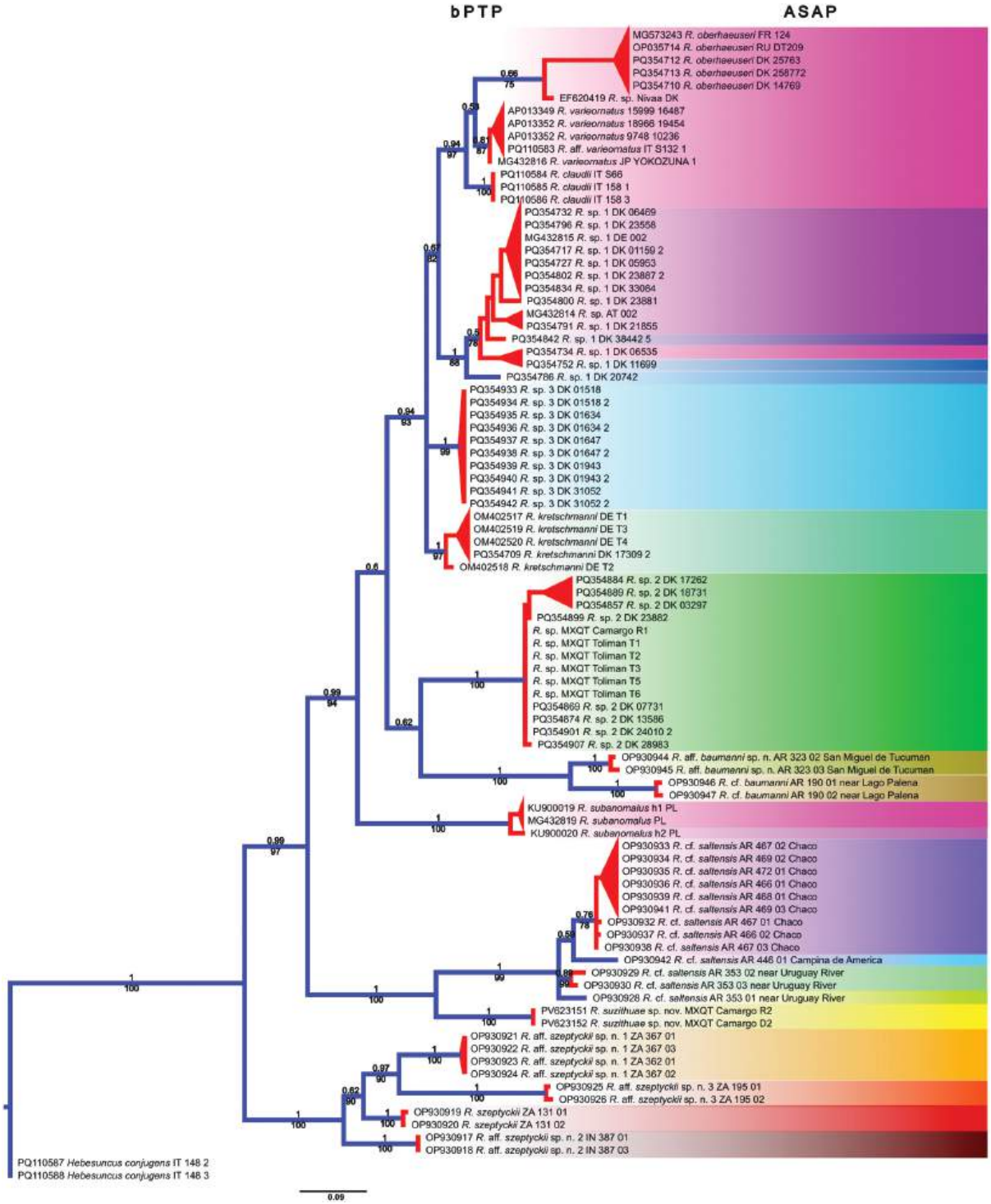

Figure 10. Molecular species delimitation of the ITS-2 sequences of the genus *Ramazzottius*. Left: putative species from the PTP analysis are indicated by transitions from blue-coloured branches to red-coloured branches. Right: different coloured sets denote specimens grouped by the best partition of the ASAP analysis. Posterior probability and bootstrap values are shown above and below branches, respectively.

Clade D. Comprises the *szeptycki* complex, divided into the subclades DA (*Ramazzottius szeptycki* + *R.* aff. *szeptycki* sp. n. 2) and DB (*R.* aff. *szeptycki* sp. n. 1 + *R.* aff. *szeptycki* sp. n. 3).

Clade X. Constituted by *Ramazzottius* aff. *oberhaeuseri* sp. 4 and *R.* aff. *oberhaeuseri* sp. 5, this clade is so named because its position was variable among clades (Supporting information S4). This is likely due to the

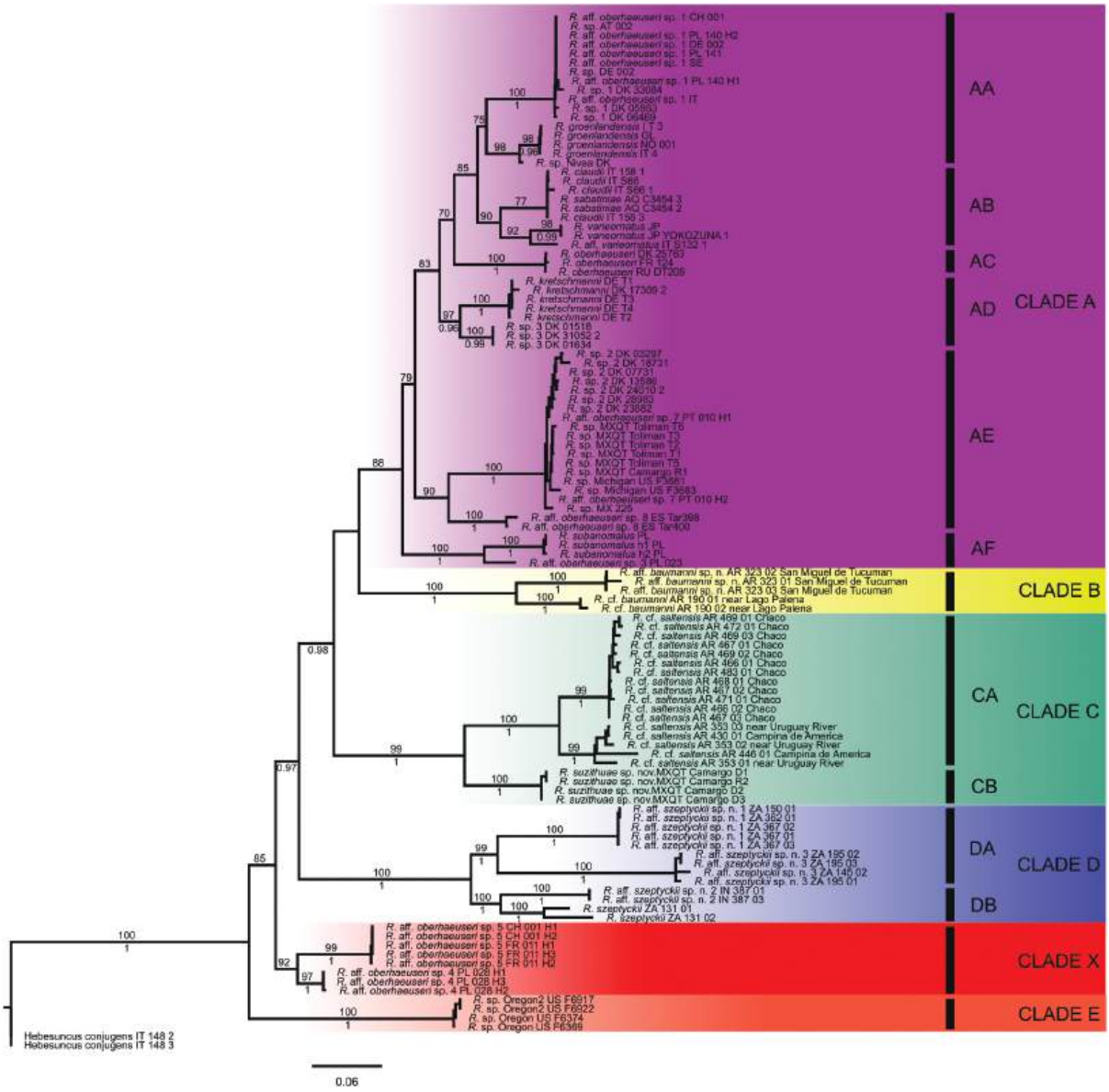

Figure 11. Phylogenetic inference of the thinned COI + ITS-2 + 28S + 18S matrix of the genus *Ramazzottius* reconstructed with ML and BI analyses. Different colours denote each major clade, while vertical bars and two-letter labels denote subclades when present. Bootstrap and posterior probability values are presented above and below the branches, respectively. Only bootstrap values ≥70% and posterior probability values ≥0.95 are shown.

lack of any more conserved marker than COI for these species. When this clade is also pruned, the topology is maintained and most of the support values of the major clades increase (Supporting information S4.6–7).

Clade E. Comprises the most basal species of all the multi-locus sequenced specimens available for the genus *Ramazzottius*, but it has no associated morphological data.

Discussion

Single-locus trees and species delimitation

The species delimitation with the COI marker is mostly consistent with current taxonomy of the *Ramazzottius* genus (Guidetti et al. 2022; Kihm et al. 2023; Vecchi & Stec 2024), with the exceptions of over-splits in *Ramazzottius* sp. 8 and *Ramazzottius* cf. *saltensis* from Campiña de América + Near Uruguay River in bPTP, as

well as *R. szeptycki* from the same sample in both analyses. This was most likely due to the large number of ambiguous bases in these sequences.

Well-supported clades above the species level in the COI phylogeny suggest closely related species, as COI exhibits good resolution in this rank, but little deeper phylogenetic signal (Rubinoff & Holland 2005; Doorenweerd et al. 2024), so that the support of deeper nodes should not be considered.

On the other hand, the topology of the ITS-2 tree was partially similar to that inferred with concatenated data in previous studies (Dey et al. 2023), illustrating the deeper phylogenetic resolution and representativeness of the ITS-2 marker with respect to COI. However, although ITS-2 was highlighted as a useful tool even for intraspecific distinction (Stec et al. 2016), its performance for species delimitation was ambiguous and incongruent with respect to COI delimitation and even between ASAP and bPTP analyses. Over-splits of *Ramazzottius* cf. *saltensis* from Campiña de América + Near Uruguay River and *Ramazzottius* sp. 1 from Denmark were recovered despite the low number of ambiguous bases.

At the same time, ITS-2 failed to delimit known different species that were clearly separated with the COI gene, like the cluster *Ramazzottius subanomalus* + *R. claudii* + *R. varieornatus* + *R. oberhaeuseri s.s.* in the ASAP partition or *Ramazzottius* aff. *varieornatus* + *R. varieornatus* in both delimitation analyses.

The congruent bPTP delimitation recovered subsets detected in COI delimitation such as the inclusion of a Russian population to *R. oberhaeuseri s.s.* and the split of *R.* cf. *saltensis* from Chaco and Campiña de América + Near Uruguay River into at least two different PSH, strongly suggesting that the *Ramazzottius* cf. *saltensis* are actually two or more sibling species within their own complex, splitting the *baumanni* complex *sensu* Dey et al. (2023). This confusion recalls statements of Pilato (2024) on the prevailing importance of adequate morphological characterization and diagnosis accompanying molecular data to increase the consistency of species delimitation in an integrative taxonomy framework.

Rethinking the COI role?

Recently, Gąsiorek et al. (2024) used ITS-2 as a primary barcoding tool, leaving COI in the background. COI displays high support values at the level of closely related species and below, but as expected for a highly variable marker, the support of more internal nodes plummets. In contrast, the ITS-2 fragments usually recover better supported internal and external nodes, although in this study it failed to distinguish closely related species such as *Ramazzottius* aff. *varieornatus* and *R. varieornatus*.

In any case, alternatives to alleviate the lack of depth provided by the COI fragment without neglecting mitochondrial information go from adding more mitochondrial markers with different rates of evolution to compensate COI's performance, to dramatically shifting the use of the COI gene to more representative regions of the mitochondrial genome.

Firstly, markers such as mitochondrial rRNA 12S and 16S have been considered better in the resolution of molecular systematics, comparable to the 18S and 28S nuclear rRNA genes (Chan et al. 2021). Secondly, changing COI for another marker should be evaluated in depth, since it is highly recommended to first assess which genes could represent more closely the full mitogenome phylogeny (Havird & Santos 2014; Main et al. 2024), and such an approach has never been carried out in the Phylum Tardigrada.

In our opinion, the use of mitochondrial markers should not be neglected. COI, for instance, still shows good support for closely related species and a better performance in molecular species delimitation than ITS-2, making it suitable for studies with correctly delimited context and taxa (Rubinoff & Holland 2005; Menezes et al. 2024; Doorenweerd et al. 2024). We also suggest that regardless of the choice of molecular marker to delimit species, it is always desirable to add as much information as possible; that is, sequencing several loci, both mitochondrial and nuclear, is ideal to obtain more information that complements and serves for the comparison of species (Padial et al. 2010).

Deeper research on these topics is desirable, since the concordance of mitochondrial and nuclear topologies have never been evaluated in tardigrades and a handful of phenomena can influence them differentially, such as the presence of polyploidy and sperm-dependent asexual species, markers of different inheritance dynamics, introgression, ancient hybridization events, secondary breaches of reproductive

barriers or incomplete lineage sorting (Rebecchi & Bertolani 1988; Toews & Brelsford 2012; Poroshina et al. 2020; Janko et al. 2023; Villegas et al. 2024).

Multi-locus phylogeny

Clade A includes *Ramazzottius oberhaeuseri s.s.* and the most widely distributed species known to date in the genus (*Ramazzottius* aff. *oberhaeuseri* sp. 7). Although it encompasses the most closely related species to the neotype species of the genus, Clade A does not have consistent diagnostic traits. The dorsal sculpture ranges from smooth (*Ramazzottius kretschmanni*, *R. subanomalus*) to "strongly sculptured" (*Ramazzottius* aff. *oberhaeuseri* spp. 1 and 7) as evidenced since the study of Stec et al. (2018). Even the well supported subclade AF includes species with very different egg morphology (e.g. hemispherical processes in *Ramazzottius* aff. *oberhaeuseri* sp. 3 and small to minute conical processes in *R. subanomalus*) despite both species having a smooth dorsal cuticle.

In fact, the similarity between eggs of *Ramazzotius claudii* (Clade A) and *R. suzithuae* sp. nov. (Clade C) suggests that eggs evolving separately could converge to a similar morphology in distant clades. Hence, this homoplasy could prevent reliable identifications based solely on egg morphology.

This need to provide descriptions with sufficient information on animals and eggs is illustrated in the *baumanni* clade (Clade B), for which there is no information on the egg morphology and the dorsal sculpture can be confused with that of the *saltensis* clade (e.g. with some adults of *R. suzithuae*), preventing a conclusive morphological diagnosis despite their evident molecular distinction.

Similarly, the *szeptycki* clade (Clade D) has a unique cuticular sculpture and body shape (Dey et al. 2023); however, declaring this clade in a further nomenclatural act (e.g. erecting a new genus) requires, at least, information on the egg morphology, totally unknown to date.

A clade comprising a true *oberheuseri* complex remains elusive, corresponding only to a morphogroup, as noted by Kihm et al. (2023), since *Ramazzottius oberhaeuseri s.s.* does not cluster with any other species in our analysis nor in any previous multilocus phylogeny (Guidetti et al. 2019; Dey et al. 2023; Kihm et al. 2023; Vecchi & Stec 2024).

Knowing that the recognized clades could eventually become different genera when enough diagnostic information is available (even encompassing more than one genus within Clade A based on its variability), the premature inclusion of the *Cryoconicus* species (from a still paraphyletic genus) within *Ramazzottius* could double the work, as *Cryoconicus* species are located externally to the whole Clade A in the present study (as suggested by the analysis in Dey et al. 2023). Therefore, the current *Cryoconicus* species would not be a part of *Ramazzottius s.s.*, but they are closer to what *Ramazzottius s.s.* is likely to be than Clades B–E.

Clade B in Dey et al. (2023) is consistently positioned as the most basal group in our analysis (Clade E). Not so the positioning of *Ramazzottius* aff. *oberhaeuseri* sp. 4 and 5, so it is necessary to survey their localities again and integrate more morphological and molecular information to unveil their affinities within *Ramazzottius*.

In Clade E, the inclusion of short conservative single-locus sequences clusters specimens from Alaska within this species (Supporting information S4.1–2), but more variable markers are needed to confirm the relationship between these specimens.

Additional taxonomical comments

Considering that *Ramazzottius* cf. *saltensis* from Argentina (Dey et al. 2023) most probably comprises two different species, it is important to note that the PhC and SEM images provided by Dey et al. (2023; Figures 2 and 3) correspond to specimens only from Chaco.

Even if differences in a particular stage of life have not been previously stressed in *Ramazzottius*, *R. suzithuae* sp. nov. showed that potentially ontogenetic changes can occur in the genus (Figure 3). This brings new questions on morphological records based only on one life stage and/or a reduced number of specimens. An immediate example comes from a species morphologically similar to *R. suzithuae* sp. nov: *Ramazzottius belubellus* Bartels et al. 2011. Hence, there is a possibility that the other *Ramazzottius* specimens reported by Bartels et al. (2011), attributed to *R. baumanni*, were adults of *R. belubellus* with flattened spines, especially considering the small size of the type series. However, this assumption requires revision of the original material and obtaining more animals for DNA amplification, a hard task given the low abundance and frequency reported for the species.

An additional problematic this study would like to address is the fact that most of the Neotropical records have been historically associated with Holarctic species and considered therefore widely distributed or cosmopolitan ("False cosmopolitan records" in Ugarte & Garraffoni 2024) with only limited morphological evidence. To break through this issue, it is important to revisit morphological records in the Neotropics and generate molecular data, at least for the more variable markers such as COI and ITS-2, as well as trying to include this information in every description of a new species.

A very interesting example of the consequences in this matter is a Brazilian record reported as "*Ramazzottius oberhaeuseri*" (De Barros 1943), even though the morphology of the cuticle is completely different from the species publicly known at that time, and even today, consisting of a dense granulation on the entire dorsal cuticle, accompanied by five rows of four gibbosities from the first to the third pair of legs. Specimens with similar characteristics have been found in the Mexican state of Hidalgo (in prep., Supporting information S5), suggesting that the drawings of "*Ramazzottius oberhaeuseri*" in De Barros (1943) may not be an exaggerated mistake, but a true extant new species.

At the same time, poorly detailed descriptions can obscure the actual validity of some species, as occurred with *Ramazzottius edmondabouti* Séméria 1993, considered *species dubia* (Guidetti et al. 2022) due to its vague original description. However, specimens with a very similar dorsal sculpture (polygonal tubercles with sclerotized apices present on the dorsum except for segments I–II and the medial portion of segments IV, VI, VIII and X) have been found in Mexico (in prep., Supporting information S5), thence we consider that the status of *species dubium* for *R. edmondabouti* should be revoked or changed to *species inquirenda*, since its poor description hinder comparative analysis, but still shows morphological novelty in the dorsal sculpture, unseen in the rest of formally described species in the genus.

Additionally, according to the phylogenetic reconstruction, *Ramazzottius suzithuae* sp. nov belongs to a broader "*baumanni*" morphogroup (but not strictly a complex *sensu* Dey et al. 2023) and forms a monophyletic clade with at least two more species, previously thought to be a single species (*Ramazzottius* cf. *saltensis* in Dey et al. 2023). Since *R. belubellus* has the most similar dorsal sculpture to that of the new species, it is probable that it is more closely related to the "*saltensis*" clade C. Finally, *Ramazzottius theroni* is similar to the new species, in both its sculpture and its eggs (Dastych 1993), so we consider including it in the *baumanni* morphogroup, extending its distribution far beyond the Neotropics, but await available information on the egg morphology of the *baumanni* clade B to better understand its differences from the *saltensis* clade C.

Conclusions

A new species from Mexico, *Ramazzottius suzithuae* sp. nov., is described and molecularly delimited from other species with both ASAP and bPTP analysis. Moreover, its discovery evidences the existence of a separate clade hidden in the previously suggested "*baumanni*" complex, encompassing at least two species formerly identified as *Ramazzottius* cf. *saltensis* and the new species. The phylogeny of the genus *Ramazzottius* shows its complex nature, requiring comprehensive examination in future research.

Acknowledgments

This paper is part of the requirements for obtaining a Doctoral degree at the Posgrado en Ciencias Biológicas, UNAM, for Jorge Romero-Mendoza. Thanks to the Secretaría de Ciencia, Humanidades, Tecnología e Innovación, SECIHTI (previously CONAHCYT), for the grant to Jorge Romero-Mendoza (CVU No. 921536). Special thanks to Laura Gómez for her always kind assistance in obtaining SEM images at the Institute of Marine Sciences and Limnology, UNAM. We appreciate the kindness of Jorge Jiménez in providing the old moss and lichen samples. We are grateful for the services of the Laboratorio Nacional de Biodiversidad (LaNaBio, UNAM), such as the infrastructural support provided by Berenit Mendoza (PhC images) and by Andrea Jiménez-Marín, Nelly López, and Laura Márquez (DNA extraction, amplification, and sequencing). Last but not least, Daniel López-Sandoval is heartily thanked for lending primer aliquots for the COI and 18S markers and for all his friendly advice, tips and chats on varied tardi-topics.

Disclosure statement

No potential conflict of interest was reported by the author(s).

Funding

The project was partially funded under the National Recovery and Resilience Plan (NRRP), Mission 4 Component 2 Investment 1.4–Call for tender No. 3138 of 16 December 2021, rectified by Decree no. 3175 of 18 December 2021 of the Ministero dell'Università e della Ricerca, [CUP E93C22001090001] funded by the European Union, Award Number: [Project Code CN_00000033], Project Title 'National Biodiversity Future Center–NBCF'.

ORCID

J. Romero-Mendoza http://orcid.org/0009-0002-8348-9317
S. Brandoli http://orcid.org/0009-0000-1930-6649
R. Guidetti http://orcid.org/0000-0001-6079-2538
J. Vincenzi http://orcid.org/0009-0009-7924-4975
D. Hérnandez-Mena http://orcid.org/0000-0003-0822-3498
M. Cesari http://orcid.org/0000-0001-8857-3791
R. Mata-López http://orcid.org/0000-0002-2411-7604
G. Rivas http://orcid.org/0000-0003-0075-5609

References

Altschul SF, Gish W, Miller W, Myers EW, Lipman DJ. 1990. Basic local alignment search tool. Journal of Molecular Biology 215(3):403–410. DOI: 10.1016/S0022-2836(05)80360-2.

Bartels PJ, Nelson DR, Kaczmarek Ł, Michalczyk Ł. 2011. *Ramazzottius belubellus*, a new species of Tardigrada (Eutardigrada: Parachela: Hypsibiidae) from the Great Smoky Mountains National Park (North Carolina, USA). Proceedings of the Biological Society of Washington 124(1):3–27. DOI: 10.2988/10-13.1.

Beasley CW. 1972. Some tardigrades from Mexico. The Southwestern Naturalist 17(1):21–29. DOI: 10.2307/3669835.

Beasley CW, Kaczmarek Ł, Michalczyk Ł. 2008. *Doryphoribius mexicanus*, a new species of Tardigrada (Eutardigrada: Hypsibiidae) from Mexico (North America). Proceedings of the Biological Society of Washington 121(1):34–40. DOI: 10.2988/07-30.1.

Bertolani R, Kinchin IM. 1993. A new species of *Ramazzottius* (Tardigrada, Hypsibiidae) in a rain gutter sediment from England. Zoological Journal of the Linnean Society 109(3):27–333. DOI: 10.1111/j.1096-3642.1993.tb02538.x.

Binda MG, Pilato G. 1986. *Ramazzottius*, Nuovo Genere Di Eutardigrado (Hypsibiidae). Animalia 13:159–166.

Binda MG, Pilato G. 1994. Notizie sui Tardigradi delle Isole Hawaii con descrizione di due specie nuove. Animalia 21(1/3):57–62.

Biserov VI. 1985. *Hypsibius subanomalus* sp. n. (Eutardigrada, Hypsibiidae) from the Astrakhan district. Zoologichesky Zhurnal 64(1):131–135.

Biserov VI, Tumanov DV. 1993. *Ramazzottius valaamis* sp. n. (Tardigrada, Hypsibiidae), a new species of tardigrads from Valaam Island, Karelia, Russia. Zoologicheskii Zhurnal 72:35–39.

Camarda D, Massa E, Guidetti R, Lisi O. 2024. A new, simplified, drying protocol to prepare tardigrades for scanning electron microscopy. Microscopy Research and Technique 87(4):716–726. DOI: 10.1002/jemt.24460.

Chan AHE, Chaisiri K, Saralamba S, Morand S, Thaenkham U. 2021. Assessing the suitability of mitochondrial and nuclear DNA genetic markers for molecular systematics and species identification of helminths. Parasites and Vectors 14(1):233. DOI: 10.1186/s13071-021-04737-y.

Chernomor O, Von Haeseler A, Minh BQ. 2016. Terrace aware data structure for phylogenomic inference from supermatrices. Systematic Biology 65(6):997–1008. DOI: 10.1093/sysbio/syw037.

Dastych H. 1993. A new genus and four new species of semiterrestrial water-bears from South Africa (Tardigrada). Mitteilungen aus dem Zoologischen Museum Institute 90:175–186.

De Barros R. 1943. Tardígrados do Estado de Sao Paulo, Brazil. III. *Hypsibius, Itaquascon*, and *Milnesium* genera. Revista brasileira de biologia 3:1–10.

Degma P, Guidetti R. 2025. Actual checklist of Tardigrada species. 44th ed. University of Modena and Reggio Emilia. DOI: 10.25431/11380_1178608. Accessed May 2025 30.

Dey PK, López-López A, Morek W, Michalczyk Ł. 2023. Tardigrade *Augean stables*—A challenging phylogeny and taxonomy of the family Ramazzottiidae (Eutardigrada: Hypsibioidea). Zoological Journal of the Linnean Society 200(1):95–110. DOI: 10.1093/zoolinnean/zlad161.

Doorenweerd C, SanJose M, Leblanc L, Barr N, Geib SM, Chung AYC, Dupuis JR, Ekayanti A, Fiegalan E, Hemachandra KS, Hossain MA, Huang CL, Hsu YF, Morris KY, Mustapeng AMA, Niogret J, Pham TH, Nguyen NT, Sirisena UGAI, Todd T, Rubinoff D. 2024. Towards a better future for DNA barcoding: Evaluating monophyly- and distance-based species identification using COI gene fragments of Dacini fruit flies. Molecular Ecology Resources 24(6):e13987. DOI: 10.1111/1755-0998.13987.

Doyère L. 1840. Mémoire sur les Tardigrades. Annales des sciences naturelles. Ser. 2 Paris 14:269–361.

Folmer O, Black M, Hoeh W, Lutz R, Vrijenhoek R. 1994. DNA primers for amplification of mitochondrial cytochrome c oxidase subunit I from diverse metazoan invertebrates. Molecular Marine Biology and Biotechnology 3(5):294–299.
Gąsiorek P, Sørensen MV, Lillemark MR, Leerhøi F, Tøttrup AP. 2024. Massive citizen science sampling and integrated taxonomic approach unravel Danish cryptogam-dwelling tardigrade fauna. Frontiers in Zoology 21(1):27. DOI: 10.1186/s12983-024-00547-x.
Gąsiorek P, Stec D, Morek W, Michalczyk Ł. 2018. An integrative redescription of *Hypsibius dujardini* (Doyère, 1840), the nominal taxon for Hypsibioidea (Tardigrada: Eutardigrada). Zootaxa 4415(1):45–75. DOI: 10.11646/zootaxa.4415.1.2.
Goldstein PZ, DeSalle R. 2011. Integrating DNA barcode data and taxonomic practice: Determination, discovery, and description. BioEssays 33(2):135–147. DOI: 10.1002/bies.201000036.
Guidetti R, Bertolani R. 2005. Tardigrade taxonomy: An updated checklist of the taxa and a list of characters for their identification. Zootaxa 845(1):1–46. DOI: 10.11646/zootaxa.845.1.1.
Guidetti R, Cesari M, Giovannini I, Ebel C, Förschler MI, Rebecchi L, Schill RO. 2022. Morphology and taxonomy of the genus *Ramazzottius* (Eutardigrada; Ramazzottiidae) with the integrative description of *Ramazzottius kretschmanni* sp. nov. European Zoological Journal 89(1):346–370. DOI: 10.1080/24750263.2022.2043468.
Guidetti R, Massa E, Bertolani R, Rebecchi L, Cesari M. 2019. Increasing knowledge of Antarctic biodiversity: New endemic taxa of tardigrades (Eutardigrada; Ramazzottiidae) and their evolutionary relationships. Systematics & Biodiversity 17(6):573–593. DOI: 10.1080/14772000.2019.1649737.
Havird JC, Santos SR. 2014. Performance of single and concatenated sets of mitochondrial genes at inferring metazoan relationships relative to full mitogenome data. PLOS ONE 9(1):e84080. DOI: 10.1371/journal.pone.0084080.
Hernández-Mena DI, Cabañas-Granillo J, Medina-Hernández E, Pérez-Ponce de León G. 2022. Discovery of a new species of *Homalometron* Stafford, 1904 (Digenea: Apocreadiidae) from the stripped mojarra, *Eugerresplumieri* in a coastal lagoon of the Gulf of Mexico. Journal of Helminthology 96:e46. DOI: 10.1017/S0022149X22000372.
Hoang DT, Chernomor O, Von Haeseler A, Minh BQ, Vinh LS. 2018. UFBoot2: Improving the ultrafast bootstrap approximation. Molecular Biology and Evolution 35(2):518–522. DOI: 10.1093/molbev/msx281.
Inkscape Project. 2020. Inkscape. https://inkscape.org.
Janko K, Mikulíček P, Hobza R, Schlupp I. 2023. Sperm-dependent asexual species and their role in ecology and evolution. Ecology and Evolution 13(10):e10522. DOI: 10.1002/ece3.10522.
Kaczmarek Ł, Michalczyk Ł. 2017. The *Macrobiotus hufelandi* group (Tardigrada) revisited. Zootaxa 4363(1):101–123. DOI: 10.11646/zootaxa.4363.1.4.
Kaczmarek Ł, Michalczyk Ł, McInnes SJ. 2014. Annotated zoogeography of non-marine Tardigrada. Part I: Central America. Zootaxa 3763(1):1–62. DOI: 10.11646/zootaxa.3763.1.1.
Kalyaanamoorthy S, Minh BQ, Wong TK, Von Haeseler A, Jermiin LS. 2017. ModelFinder: Fast model selection for accurate phylogenetic estimates. Nature Methods 14(6):587–589. DOI: 10.1038/nmeth.4285.
Katoh K, Misawa K, Kuma KI, Miyata T. 2002. MAFFT: A novel method for rapid multiple sequence alignment based on fast fourier transform. Nucleic Acids Research 30(14):3059–3066. DOI: 10.1093/nar/gkf436.
Kihm JH, Zawierucha K, Rho HS, Park TYS. 2023. Homology of the head sensory structures between Heterotardigrada and Eutardigrada su pported in a new species of water bear (Ramazzottiidae: *Ramazzottius*). Zoological Letters 9(1):22. DOI: 10.1186/s40851-023-00221-w.
Kumar S, Stecher G, Tamura K. 2016. MEGA7: Molecular evolutionary genetics analysis version 7.0 for bigger datasets. Molecular Biology and Evolution 33(7):1870–1874. DOI: 10.1093/molbev/msw054.
López-Sandoval D, Montiel-Parra G, Pérez TM. 2025. New records of tardigrades from Mexico with the description of *Paramacrobiotus puma* sp. nov. (Eutardigrada: Macrobiotidae). Revista Mexicana De Biodiversidad 96:e965488. DOI: 10.22201/ib.20078706e.2025.96.5488.
Luton K, Walker D, Blair D. 1992. Comparison of ribosomal internal transcribed spacer from two congeneric species of flukes (Platyhelminthes: Trematoda: Digenea). Molecular and Biochemical Parasitology 56(2):323–328. DOI: 10.1016/0166-6851(92)90181-I.
Madeira F, Madhusoodanan N, Lee J, Eusebi A, Niewielska A, Tivey AR, Lopez R, Butcher S. 2024. The EMBL-EBI Job dispatcher sequence analysis tools framework in 2024. Nucleic Acids Research 52(W1):W521–W525. DOI: 10.1093/nar/gkae241.
Magoga G, Fontaneto D, Montagna M. 2021. Factors affecting the efficiency of molecular species delimitation in a species-rich insect family. Molecular Ecology Resources 21(5):1475–1489. DOI: 10.1111/1755-0998.13352.
Main DC, Taft JM, Geneva AJ, Vuuren BJ, Tolley KA. 2024. The efficacy of single mitochondrial genes at reconciling the complete mitogenome phylogeny—A case study on dwarf chameleons. PeerJ 12:e17076. DOI: 10.7717/peerj.17076.
McInnes SJ, Michalczyk Ł, Kaczmarek Ł. 2017. Annotated zoogeography of non-marine Tardigrada. Part IV: Africa. Zootaxa 4284(1):1–74. DOI: 10.11646/zootaxa.4284.1.1.
Menezes RS, Noll FB, Aragão M, Hermes MG, Brady SG. 2024. Phylomitogenomics reveals mito-nuclear concordance in social wasps: The performance of mitochondrial markers and gene order for hymenopteran systematics. Systematic Entomology 49(1):15–27. DOI: 10.1111/syen.12604.
Michalczyk Ł, Kaczmarek Ł. 2010. Description of *Doryphoribius dawkinsi*, a new species of Tardigrada (Eutardigrada: Hypsibiidae) from the Costa Rican highlands, with the key to the genus *Doryphoribius*. Zootaxa 2393(1):46–58. DOI: 10.11646/zootaxa.2393.1.4.
Michalczyk Ł, Kaczmarek Ł. 2013. The Tardigrada register: A comprehensive online data repository for tardigrade taxonomy. Journal of Limnology 72(1s):175–181. DOI: 10.4081/jlimnol.2013.s1.e22.

Michalczyk Ł, Kaczmarek Ł, McInnes SJ. 2022. Annotated zoogeography of non-marine Tardigrada. Part V: Australasia. Zootaxa 5107(1):1–119. DOI: 10.11646/zootaxa.5107.1.1.

Michalczyk Ł, Wełnicz W, Frohme M, Kaczmarek Ł. 2012. Redescriptions of three *Milnesium* Doyère, 1840 taxa (Tardigrada: Eutardigrada: Milnesiidae), including the nominal species for the genus. Zootaxa 3393(1):66–68. DOI: 10.11646/zootaxa.3154.1.1.

Mironov SV, Dabert J, Dabert M. 2012. A new feather mite species of the genus *Proctophyllodes* Robin, 1877 (Astigmata: Proctophyllodidae) from the long-tailed Tit *Aegithalos caudatus* (Passeriformes: Aegithalidae)—morphological description with DNA barcode data. Zootaxa 3253(1):54–61. DOI: 10.11646/zootaxa.3253.1.2.

Montero-Pau J, Gómez A, Muñoz J. 2008. Application of an inexpensive and high-throughput genomic DNA extraction method for the molecular ecology of zooplanktonic diapausing eggs. Limnology and Oceanography: Methods 6 (6):218–222. DOI: 10.4319/lom.2008.6.218.

Moreno-Talamantes A, Roszkowska M, García-Aranda MA, Flores-Maldonado JJ, Kaczmarek Ł. 2019. Current knowledge on Mexican tardigrades with a description of *Milnesium cassandrae* sp. nov. (Eutardigrada: Milnesiidae) and discussion on the taxonomic value of dorsal pseudoplates in the genus *Milnesium* Doyère, 1840. Zootaxa 4691(5):501–524. DOI: 10.11646/zootaxa.4691.5.5.

Nadler SA, Hudspeth DSS. 1998. Ribosomal DNA and phylogeny of the Ascaridoidea (Nemata: Secernentea): Implications for morphological evolution and classification. Molecular Phylogenetics and Evolution 10(2):221–236. DOI: 10.1006/mpev.1998.0514.

Nguyen LT, Schmidt HA, Von Haeseler A, Minh BQ. 2015. IQ-TREE: A fast and effective stochastic algorithm for estimating maximum-likelihood phylogenies. Molecular Biology and Evolution 32(1):268–274. DOI: 10.1093/molbev/msu300.

Padial JM, Miralles A, De la Riva I, Vences M. 2010. The integrative future of taxonomy. Frontiers in Zoology 7(1):Article 16. DOI: 10.1186/1742-9994-7-16.

Pante E, Puillandre N, Viricel A, Arnaud-Haond S, Aurelle D, Castelin M, Chenuil A, Destombe C, Forcioli D, Valero M, Viard F, Samadi S. 2015. Species are hypotheses: Avoid connectivity assessments based on pillars of sand. Molecular Ecology 24(3):525–544. DOI: 10.1111/mec.13048.

Pilato G. 1969. Evoluzione e nuova sistemazione degli Eutardigrada. Bollettino di Zoologia 36(3):327–345. DOI: 10.1080/11250006909436925.

Pilato G. 1981. Analisi di nuovi caratteri nello studio degli Eutardigradi. Animalia 8:51–57.

Pilato G. 2024. Discussion on the morphological and molecular data used in the study of tardigrade systematics. Biodiversity Journal 15(4):935–955. DOI: 10.31396/Biodiv.Jour.2024.15.4.935.955.

Polishchuk A, Kayastha P, Młodzianowska D, Michalska M, Gawlak M, Warguła J, Kaczmarek Ł. 2025. Description of two new species and a new population of *Mesobiotus* cf. *coronatus* from Cotacachi-Cayapas National Park, Ecuador. PLOS ONE 20(6):e0324518. DOI: 10.1371/journal.pone.0324518.

Poroshina AA, Sherbakov DY, Peretolchina TE. 2020. Diagnosis of the mechanisms of different types of discordances between phylogenies inferred from nuclear and mitochondrial markers. Vavilovskii zhurnal genetikiiselektsii 24 (4):420–426. DOI: 10.18699/VJ20.634.

Prendini L, Weygoldt P, Wheeler WC. 2005. Systematics of the *Damon variegatus* group of African whip spiders (Chelicerata: Amblypygi): Evidence from behaviour, morphology and DNA. Organisms Diversity & Evolution 5 (3):203–236. DOI: 10.1016/j.ode.2004.12.004.

Puillandre N, Brouillet S, Achaz G. 2021. ASAP: Assemble species by automatic partitioning. Molecular Ecology Resources 21(2):609–620. DOI: 10.1111/1755-0998.13281.

Ramazzotti G. 1962. Tardigradi del Cile, con descrizione di quattro nuove specifiche di una nuova varietà. Atti Della Società Italiana Di Scienze Naturali e Del Museo Civico Di Storia Naturale in Milano 101:275–287.

Rambaut A 2007. FigTree, a graphical viewer of phylogenetic trees. http://tree.bio.ed.ac.uk/software/figtree/.

Rebecchi L, Bertolani R. 1988. New cases of parthenogenesis and polyploidy in the genus *Ramazzottius* (Tardigrada, Hypsibiidae) and a hypothesis concerning their origin. International Journal of Invertebrate Reproduction and Development 14(2–3):187–196. DOI: 10.1080/01688170.1988.10510377.

Richters F. 1926. Tardigrada. In: Kükenthal W, Krumbach T, editors. Handbuch der Zoologie. Vol. 3. Berlin & Leipzig: Walter de Gruyter & Co. pp. 1–68.

Ronquist F, Teslenko M, Van Der Mark P, Ayres DL, Darling A, Höhna S, Larget B, Liu L, Suchard MA, Huelsenbeck JP. 2012. MrBayes 3.2: Efficient Bayesian phylogenetic inference and model choice across a large model space. Systematic Biology 61(3):539–542. DOI: 10.1093/sysbio/sys029.

Rubinoff D, Holland BS. 2005. Between two extremes: Mitochondrial DNA is neither the panacea nor the nemesis of phylogenetic and taxonomic inference. Systematic Biology 54(6):952–961. DOI: 10.1080/10635150500234674.

Sands CJ, McInnes SJ, Marley NJ, Goodall-Copestake W, Convey P, Linse K. 2008. Phylum Tardigrada: An "individual" approach. Cladistics 24(6):1–18. DOI: 10.1111/j.1096-0031.2008.00219.x.

Schuster RO, Nelson DR, Grigarick AA, Christenberry D. 1980. Systematic criteria of the Eutardigrada. Transactions of the American Microscopical Society 99(3):284–303. DOI: 10.2307/3226004.

Séméria Y. 1993. Description d'uneespèce nouvelle de Tardigrade du Venezuela, *Ramazzottius edmondabouti* n. sp. (Eutardigrada, Hypsibiidae). Bulletin Mensuel de la Société Linnéenne de Lyon 62:215–216.

Stec D, Kristensen RM, Michalczyk Ł. 2020. An integrative description of *Minibiotus ioculator* sp. nov. From the Republic of South Africa with notes on *Minibiotus pentannulatus* Londoño et al. 2017 (Tardigrada: Macrobiotidae). Zoologischer Anzeiger 286:117–134. DOI: 10.1016/j.jcz.2020.03.007.

Stec D, Morek W, Gąsiorek P, Kaczmarek Ł, Michalczyk Ł. 2016. Determinants and taxonomic consequences of extreme egg shell variability in *Ramazzottius subanomalus* (Biserov, 1985) (Tardigrada). Zootaxa 4208(2):4208. DOI: 10.11646/zootaxa.4208.2.5.

Stec D, Morek W, Gąsiorek P, Michalczyk Ł. 2018. Unmasking hidden species diversity within the *Ramazzottius oberhaeuseri* complex, with an integrative redescription of the nominal species for the family Ramazzottiidae (Tardigrada: Eutardigrada: Parachela). Systematics & Biodiversity 16(4):357–376. DOI: 10.1080/14772000.2018.1424267.

Stec D, Zawierucha K, Michalczyk Ł. 2017. An integrative description of *Ramazzottius subanomalus* (Biserov, 1985 (Tardigrada) from Poland. Zootaxa 4300(3):403–420. DOI: 10.11646/zootaxa.4300.3.4.

Stock SP, Campbell JF, Nadler SA. 2001. Phylogeny of *Steinernema* Travassos, 1927 (Cephalobina: Steinernematidae) inferred from ribosomal DNA sequences and morphological characters. Journal of Parasitology 87(4):877–889. DOI: 10.1645/0022-3395(2001)087[0877:POSTCS]2.0.CO;2.

Toews DP, Brelsford A. 2012. The biogeography of mitochondrial and nuclear discordance in animals. Molecular Ecology 21(16):3907–3930. DOI: 10.1111/j.1365-294X.2012.05664.x.

Trifinopoulos J, Nguyen LT, von Haeseler A, Minh BQ. 2016. W-IQ-TREE: A fast online phylogenetic tool for maximum likelihood analysis. Nucleic Acids Research 44(1):232–235. DOI: 10.1093/nar/gkw256.

Truett GE, Heeger P, Mynatt RL, Truett AA, Walker JA, Warman ML. 2000. Preparation of PCR-quality mouse genomic DNA with hot sodium hydroxide and tris (HotSHOT). BioTechniques 29(1):52–54. DOI: 10.2144/00291bm09.

Ugarte PDS, Garraffoni ARS. 2024. Removal of historical taxonomic bias and its impact on biogeographic analyses: A case study of Neotropical tardigrade fauna. Zoological Journal of the Linnean Society 201(3):zlae091. DOI: 10.1093/zoolinnean/zlae091.

Vecchi M, Stec D. 2024. Mitogenome of a new *Ramazzottius* species (Tardigrada: Eutardigrada: Ramazzottiidae) discovered in rock pools along with its temperature and desiccation-related proteins repertoire. Organisms Diversity & Evolution 24:1–17. DOI: 10.1007/s13127-024-00662-x.

Vences M, Miralles A, Brouillet S, Ducasse J, Fedosov A, Kharchev V, Kostadinov I, Kumari S, Patmanidis S, Scherz MD, Puillandre N, Renner SS. 2021. iTaxotools 0.1: Kickstarting a specimen-based software toolkit for taxonomists. Megataxa 6(2):77–92. DOI: 10.11646/megataxa.6.2.1.

Vences M, Patmanidis S, Kharchev V, Renner SS. 2022. Concatenator, a user friendly program to concatenate DNA sequences, implementing graphical user interfaces for MAFFT and FastTree. Bioinformatics Advances 2(1):vbac050. DOI: 10.1093/bioadv/vbac050.

Villegas LI, Ferretti L, Wiehe T, Waldvogel AM, Schiffer PH. 2024. Parthenogenomics: Insights on mutation rates and nucleotide diversity in parthenogenetic *Panagrolaimus* nematodes. Ecology and Evolution 14(1):e10831. DOI: 10.1002/ece3.10831.

Yin Y, Hu Y, Shao ZK, Yao LF, Li N, Hebert PD, Xue XF. 2023. Factors affecting the accuracy of molecular delimitation in minute herbivorous mites (Acari: Eriophyoidea). Zoologica Scripta 52(5):531–542. DOI: 10.1111/zsc.12612.

Zhang J, Kapli P, Pavlidis P, Stamatakis A. 2013. A general species delimitation method with applications to phylogenetic placements. Bioinformatics 29(22):2869–2876. DOI: 10.1093/bioinformatics/btt499.